

**EXPERIMENTAL INVESTIGATION OF THE VARIATION IN THE
POTENTIAL OF SELECTED NATURAL ROCKS AS THERMAL
ENERGY STORAGE MATERIALS**

Lilian Deusdedit Kakoko

**A Dissertation Submitted in Partial Fulfilment of the Requirements for the Degree of
Master of Science in Sustainable Energy Science and Engineering of the Nelson
Mandela African Institution of Science and Technology**

Arusha, Tanzania

August, 2023

ABSTRACT

Fossil fuels cause greenhouse gas emissions and are perceived to deplete, hence the use of renewable energy is considered crucial. These renewables include the use of solar thermal energy in concentrated solar power (CSP) generation and solar drying applications. However, solar energy is intermittent, thus solved by incorporating thermal energy storage (TES) to store heat energy for future use. However, the most common weaknesses in TES materials are high cost of investment, environmentally unfriendly and are not locally available. Using natural rocks is recommended as they are readily available, affordable and efficient TES materials for solar drying applications at 40-75 °C and concentrated solar power generation at 500-600°C. Despite its generational use in thermal applications, soapstone rock has not been studied as a TES material. Moreover, site specificity has not been investigated in spite of being stated to affect the potential of rocks in TES. Therefore, this study investigates the potential of soapstone rock as a TES material, and the influence of the geological-tectonic settings. In the present study, experimental characterization of selected natural rocks namely soapstone and granite, was done to investigate their thermal properties at 20-950°C. Conclusively, soapstone rock from the Craton geo-tectonic setting had the best properties and it had the highest young's modulus, thermal capacity, thermal conductivity and had a weight loss of only 0.75 % at 900°C. At high temperatures, it did not show visible fracture. Moreover, soapstone and granite from the Craton and Usagaran geo-tectonic settings exhibit significant differences.

DECLARATION

I, Lilian Deusdedit Kakoko, do hereby declare to the Senate of the Nelson Mandela African Institution of Science and Technology that this dissertation titled "*Experimental Investigation of the Variation in the Potential of Selected Natural Rocks as Thermal Energy Storage Materials*" is my own original work and that it has neither been submitted nor being concurrently submitted for degree award in any other institution.

Lilian Deusdedit Kakoko



21/08/2023

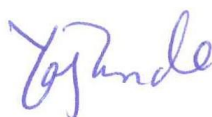
The above declaration is confirmed by:

Dr. Thomas Kivevele



21/08/2023

Prof. Yusufu Abeid Jande Chande



21/08/2023

COPYRIGHT

This dissertation is copyright material protected under the Berne Convention, the Copyright Act of 1999 and other international and national enactments, in that behalf, on intellectual property. It must not be reproduced by any means, in full or in part, except for short extracts in fair dealing; for researcher private study, critical scholarly review or discourse with an acknowledgement, without the written permission of the office of Deputy Vice Chancellor for Academics, Research and Innovations, on behalf of both the author and The Nelson Mandela African Institution of Science and Technology.

CERTIFICATION

The undersigned certify that they have read and hereby recommend for acceptance by the Senate of the Nelson Mandela African Institution of Science and Technology a dissertation titled "*Experimental Investigation of The Variation in The Potential of Selected Natural Rocks as Thermal Energy Storage Materials*" in partial fulfilment of the requirements for the Degree of Master of Science in Sustainable Energy Science and Engineering at the Nelson Mandela African Institution of Science and Technology, Arusha Tanzania.



Dr. Thomas Kivevele

21/08/2023



Prof. Yusufu Abeid Jande Chande

21/08/2023

ACKNOWLEDGMENTS

First and foremost, to Lord God, Almighty be the Glory. This work and all that I currently am is by His marvelous guidance, protection, grace and unmeasurable love.

My gratefulness to the Nelson Mandela African Institution of Science and Technology (NM-AIST) and the African Centre of Excellence for Water Infrastructure and Sustainable Energy Futures (WISE-Futures) for providing diverse support to my research. I thank my employer, Ardhi University, for the Master's degree study leave. In a special way I am truly grateful to my former Heads of Department Dr. Daniel Mbisso and Dr. Isabela Mtani, whose close guidance enabled me to successfully apply for the leave. Words shall never state the magnitude of my heartfelt appreciation to my supervisors, Dr. Thomas Kivevele and Prof. Yusufu Abeid Chande Jande, for the research funding, tremendous support, patience and continuous supervision. May God continue to bless all your endeavors in two-folds.

I am blessed beyond reason to have had the psychological and emotional support of my daughters Cecilia, Ceanna and Celisha Uiso who accompanied me during my studies at the institution. Your stay with me has truly eased my study journey. I thank my partner Mr. Joseph Uiso for his assistance in ensuring that our daughters have a comfortable childhood here in Arusha. Am forever indebted to my father Eng. Deusdedit Kakoko for not only funding my studies but also motivating me to timely pursue my postgraduate studies. I thank my aunty Ms. Leah Majigwa and my sisters Dr. Consolata Kakoko and Eng. Magreth Kakoko for their continuous intellectual and emotional support during my studies.

I value the contribution of all the staff and students in the school of MEWES for their support in molding this research through their valuable criticism during the graduate seminars and consultations. Am grateful to my friends and colleagues including Ms. Atugonza Majula, Ms. Jacqueline Uwimbabazi, Ms. Winnie Muangi, Mr. Denis Mwalongo, Mr. Paulo Chiza, Mr. Wilson Mahene, and Ms. Francisca Zakaria for their undying support in my studies and family struggles.

DEDICATION

I dedicate my entire master's degree to:

The Late JUSTINE THEODORE UISO;
my beloved father in-law

Thank you for your UNDYING LOVE, in my heart you will FOREVER LIVE.

TABLE OF CONTENTS

ABSTRACT.....	i
DECLARATION	ii
COPYRIGHT.....	iii
CERTIFICATION	iv
ACKNOWLEDGMENTS	v
DEDICATION.....	vi
TABLE OF CONTENTS.....	vii
LIST OF TABLES.....	x
LIST OF FIGURES	xi
LIST OF APPENDICES.....	xiii
LIST OF ABBREVIATIONS AND SYMBOLS	xiv
CHAPTER ONE	1
INTRODUCTION	1
1.1 Background of the Study	1
1.2 Statement of the Problem.....	3
1.3 Rationale of the Study.....	4
1.4 Research Objectives.....	4
1.4.1 Main Objective	4
1.4.2 Specific Objectives	4
1.5 Research Questions.....	5
1.6 Significance of the Study	5
1.7 Delineation of the Study	5
CHAPTER TWO	7
LITERATURE REVIEW	7
2.1 Introduction.....	7

2.2	Thermal Energy Storage	7
2.3	Materials Used for Thermal Energy Storage	7
2.3.1	Common TES Materials	8
2.3.2	Natural Rocks	10
2.4	Rocks Variations in Geo-Tectonic Settings	10
2.4.1	Archaean Craton Geo-Tectonic Setting.....	11
2.4.2	Proterozoic Geo-Tectonic Setting	11
2.5	Characterization Parameters	12
2.5.1	Thermo-Physical Properties	12
2.5.2	Thermo-Mechanical Properties	12
2.5.3	Thermo-Chemical Properties.....	13
2.6	Selected Work on Rocks as TES Materials	13
CHAPTER THREE		16
MATERIALS AND METHODS.....		16
3.1	Introduction.....	16
3.2	Materials	16
3.3	Characterisation of Rock Samples	17
3.3.1	Thermo-Chemical Properties.....	20
3.3.2	Thermo-Physical Properties	21
3.3.3	Thermo-Mechanical Properties	23
CHAPTER FOUR.....		24
RESULTS AND DISCUSSION		24
4.1	Overview	24
4.2	Thermo-Chemical Properties	24
4.2.1	Chemical Composition	24
4.2.2	Crystalline Phases.....	25

4.2.3	Structural Analysis	27
4.2.4	Thermal Gravimetric Analysis	28
4.2.5	High temperature Test	31
4.3	Thermo-Physical Properties.....	32
4.3.1	Density and Porosity.....	32
4.3.2	Specific Heat Capacity and Thermal Capacity.....	37
4.3.3	Thermal diffusivity and Conductivity	42
4.4	Thermo-Mechanical Properties.....	48
4.4.1	Young's Modulus	48
CHAPTER FIVE		50
CONCLUSION AND RECOMMENDATIONS		50
5.1	Conclusion	50
5.2	Recommendations.....	51
REFERENCES		52
APPENDICES		58
RESEARCH OUTPUTS.....		61

LIST OF TABLES

Table 1:	Common materials used for thermal energy storage and their limitations	9
Table 2:	Sample code names according to geo-tectonic setting and rock type.....	17
Table 3:	Elemental composition of soapstone rocks	25

LIST OF FIGURES

Figure 1:	Map showing the location of the collected rock samples (a) Map of Dodoma and Iringa regions showing sample collection locations and their geo-tectonic settings (b) Map of Tanzania showing the locations of Dodoma and Iringa regions (c) Map of Africa showing the location of Tanzania.....	17
Figure 2:	The characterization experiments for thermal energy storage	19
Figure 3:	Graph showing Chemical composition of US, CS, UG and CG rocks	25
Figure 4:	The XRD graphs for (a)CG, (b)UG, (c)CS and (d)US	26
Figure 5:	Petrographic image for (a)CG, (b)UG, (c)CS and (d)US.	28
Figure 6:	TGA graph for (a)CS, (b)US, (c)CG and (d)UG	30
Figure 7:	Comparison of maximum service temperature with other TES materials from literature	31
Figure 8:	Rock samples: (a) ore, (b) heated at 700°C, (C) heated at 1000°C.....	32
Figure 9:	Density and porosity at room temperature	33
Figure 10:	Comparison to the densities of other rocks from literature (Tiskatine <i>et al.</i> , 2017)	34
Figure 11:	Comparison of density with other TES materials at room temperature.....	35
Figure 12:	Evolution of density at low temperatures	36
Figure 13:	Evolution of density at high temperatures.....	36
Figure 14:	Evolution of specific heat capacity with temperature	37
Figure 15:	Comparison to the specific heat capacity of other rocks from literature (Tiskatine <i>et al.</i> , 2017).....	38
Figure 16:	Comparison of specific heat capacity with other TES materials from literature	39

Figure 17: Comparison to the specific heat capacity of other rocks from literature (Tiskatine <i>et al.</i> , 2017).....	40
Figure 18: Comparison of thermal capacity with other TES materials from literature.....	41
Figure 19: Evolution of thermal capacity at low temperatures.....	42
Figure 20: Evolution of thermal capacity at higher temperatures	42
Figure 21: Thermal diffusivity at low temperatures.....	44
Figure 22: Thermal diffusivity at high temperatures.....	44
Figure 23: Comparison to the thermal conductivities of other rocks from literature (Tiskatine <i>et al.</i> , 2017).....	45
Figure 24: Comparison of thermal conductivity with other TES materials from literature 47	
Figure 25: Thermal conductivity at low temperatures.....	48
Figure 26: Thermal conductivity at high temperatures.....	48
Figure 27: Young modulus at room temeperature.....	49

LIST OF APPENDICES

Appendix 1:	Data and Citation for the most common used TES materials.....	58
-------------	---	----

LIST OF ABBREVIATIONS AND SYMBOLS

AAS	- Atomic Absorption Spectrophotometry
ANOVA	- Analysis of variance
BET	- Brunauer-Emmett-Teller
CSP	- Concentrated Solar power
DSC	- Differential Scanning Calorimetry
FTIR	- Fourier Transform Infra-Red spectroscopy
ICP-MS	- Inductively Coupled Plasma Mass Spectrometry
ICP-OES	- Inductively Coupled Plasma Optical Emission Spectroscopy
INAA	- Neutron Activation Analysis
IR	- Infra-Red
LA-ICP-MS	- Laser Ablation Inductively Coupled Plasma Mass Spectrometry
LA-TOF-ICP-MS	- Laser Ablation Time Of Flight Inductively Coupled Plasma Mass Spectrometry
PIGE	- Particle Induced Gamma-ray Emission
PIXE	- Particle Induced X-ray Emission
SEM	- Scanning Electron Microscopy
SEM-EDS	- Scanning Electron Microscopy with Energy Dispersive Spectroscopy
TES	- Thermal Energy Storage
TGA	- Thermalgravimetric Analysis
XRD	- X-Ray Diffraction

CHAPTER ONE

INTRODUCTION

1.1 Background of the Study

Global energy demand is rapidly increasing due to the advancement in industrial activities and high rates of global population thus, necessitating the need to diversify the portfolio of world energy sources (Koçak *et al.*, 2021). The use of renewable energy technology has been said to be motivated by the perceived gradual depletion of fossil fuels reserves, their high cost and the environmental impacts from greenhouse gas emissions resulting from their application (Cabeza *et al.*, 2015; Cuce, 2018). The utilization of renewable energy reached at its peak in 2020 whereby, the employed renewable energies included bioenergy, geothermal, hydropower, ocean power, wind power and solar energy (REN21, 2021). Being the most abundant renewable energy source, clean and inexhaustible solar energy is a promising alternative to fossil fuels and can be harnessed through thermal heating, photovoltaics and concentrated thermal power (Eddemani *et al.*, 2021; REN21, 2021).

Various studies have shown that solar drying, using solar thermal energy, is an easy and affordable method of food drying. This method can ensure food security by reducing post-harvest losses of perishable products throughout the year (Suresh & Saini, 2020). Concentrated solar power (CSP) systems collect solar thermal energy at high temperature to be used for various application including the generation of electricity through thermodynamic cycles (Adeleke & Airoboman, 2019). However, solar thermal energy has limited performance due to its intermittency and unpredictability caused by the changes in the atmospheric conditions that lead to the weakening of solar irradiation, and in this episodes there is insufficient energy to run the required applications (Vindel & Polo, 2014). These limitations have led to the integration of solar thermal energy plants with thermal energy storage (TES) systems (Bal *et al.*, 2011; Kant *et al.*, 2016; Muh & Tabet, 2019).

Thermal energy storage (TES) is vital for mitigating fluctuation of solar energy, extending the energy delivery period and matching the energy demand and generation (Bal *et al.*, 2010; Kant *et al.*, 2016). The TES system is used to store heat energy that is captured from solar collectors for future use or to be transmitted it to a distant point of use. TES has proven to be an efficient and cost effective technology for applications in drying of agricultural food products at a moderate and steady temperature range, of approximately 40–76 °C (Bal *et al.*, 2010; Kant *et al.*, 2016). The TES incorporation in concentrated solar power (CSP) plants is an auspicious alternative for fossil

fuels in the developing countries since off grid areas are more widespread (Muh & Tabet, 2019). At temperatures of 500 - 600°C TES with air-rock bed has low investment cost, high reliability and efficiency, and is environmentally friendly without the need for heat exchangers (Tiskatine *et al.*, 2017) making the rocks to be a suitable TES material for both CSP generation and solar drying technology.

To improve economic viability and to overcome intermittency and unpredictability during solar drying and CSP generation, TES need to be efficient and cost effective. Therefore, a suitable material for TES should have high energy density for a higher ability to retain heat, which is a function of specific heat capacity and density, and excellent thermal conductivity for better energy transfer ability (Koçak *et al.*, 2021). High heat capacity and density will enhance the energy density, which is desirable to reduce the required storage material volume and equipment costs. Thermal conductivity should be high enough to allow heat to be transferred with a small temperature gradient from the rock's exterior surface to its core (Koçak *et al.*, 2021). The rock must have sufficient compressive strength to prevent the bottom-most layers from crushing under the weight of the rock above them (Kant *et al.*, 2016).

According to the aforementioned suitable TES material properties, rocks have been suggested as promising thermal energy storage materials (Alva *et al.*, 2017; Tiskatine *et al.*, 2017). Using rocks as a storage medium offers the potential of affordability since rocks are plentiful and inexpensive. The rocks differ in their suitability as energy storage materials (Adeleke & Airoboman, 2019). Some of the rocks that show high-energy storage potential include basalt, micro gabbro/ dolerite and granite (Allen *et al.*, 2014; El Alami *et al.*, 2020; Singh *et al.*, 2010).

Soapstone rocks have a very high thermal shock resistance than majority of natural rocks (Huhta *et al.*, 2016). Huhta *et al.* (2019) studied the composition and structure of magnesite soapstone in fire chambers construction, it was observed that the durability of the rock increased with further exposure in fire. Furthermore, soapstone rocks have been used for various thermal applications such as cooking utensils (Frink *et al.*, 2012), internal lining of ovens, fireplaces and stoves (Pirinen, 2005) and in high temperature components of electrical appliances (Kora, 2020). Due to these afore-mentioned excellent thermal properties, it is relevant to investigate soapstone rocks' potential as TES materials. Additionally, even rocks of a particular type may exhibit different properties depending on their mineralogical variations, thus potentially affecting their suitability for energy storage application (Adeleke & Airoboman, 2019; El Alami *et al.*, 2020). Nahhas *et al.* (2019) conducted experimental characterization on basalt rocks from France and Egypt, whereby the two rocks showed a variation in the thermal energy storage potential whereby, the basalt from France had desirable properties as opposed to the basalt from Egypt. Moreover, the study by

Bouvry *et al.* (2017) showed that primitive basalt rocks from Spain and France could perform well as thermal energy storage materials as opposed to the evolved basalts from Egypt and Greece. Tiskatine *et al.* (2017) conducted a thermal cycling tests and thermo-physical and mechanical experiments rhyolite, rock types the results concluded that the thermal energy storage parameters substantially vary in a rock of a similar type. Rock variability is caused by factors such as disjointedness conditions, characteristics of the formative materials, eon and weathering and climatic conditions (Aladejare & Wang, 2016), these factors are also dependent on geological tectonic settings.

Globally, granites are the most abundant rocks throughout the continental crust, they are most widespread and come in a variety of properties including chemical composition and grain sizes (Allen *et al.*, 2014; Halder & Tišljarić, 2014) hence are expected to be most widespread across a diverse range of geo-tectonic settings. Granite has also been recommended as an energy storage material, for example, Shang *et al.* (2019) measured the evolution of mineral composition, pore structure, and mechanical structure at a temperature range of 25°C to 1200°C and suggested that granite rocks are potential TES material in systems of up to 800°C since until this temperature the chemical and mineralogical compositions showed significant stability. Hence, this study examines the suitability of soapstone and granite rocks from two different geological settings in Tanzania, as medium for TES for solar drying and CSP generation application. The effect of structural and compositional variations of specific rock types on their suitability for thermal energy storage capacity application will be evaluated.

1.2 Statement of the Problem

Although solar energy is abundant, clean and inexhaustible it has a challenge of intermittence and unpredictability. Solar energy is time and weather dependent, causing energy loss during excessive radiation and energy unavailability during weakened radiation. The integrated of thermal energy storage (TES) system intends to mitigate the impacts of the intermittent nature of solar radiation. TES stores excess thermal energy and provide a supply when solar energy is insufficient, thus minimizing the gap between energy supply and demand. In solar drying applications so as to enhance food security and concentrated solar power (CSP) plants for electric power generation, rocks have been identified to be TES materials with potential thermo-physical, mechanical, and chemical properties for TES at low and medium temperatures. Rocks have been found to be efficient and cost effective TES materials for applications in drying of perishable agricultural products at a moderate and steady temperature of around 40–75°C. TES incorporation in concentrated solar power (CSP) plants at temperatures of 500 – 600°C with air-rock bed has low investment cost, high reliability and efficiency, environmentally friendliness without the use of

heat exchangers (Tiskatine *et al.*, 2017). To be used as a TES material, the rocks need to have good thermal properties including chemical stability at elevated temperatures, high mechanical strength, high thermal capacity and conductivity. Despite the fact that soapstone rocks have been used for various thermal applications such as cooking utensils, internal lining of ovens, fireplaces, stoves and in thermal components of electronic devices, it has not been studied as a thermal energy storage material. Additionally, rock properties have been mentioned to vary spatially and the performance of natural rocks as TES materials is known to be site specific (Adeleke & Airoboman, 2019). Nevertheless, studies have not been conducted to study the variations in the potential of the rocks according to the geological tectonic setting of origin. Since granite is among the most abundant rocks globally thus highly spread in a variety of geo-tectonic settings, it will be used together with soapstone in this study. The study therefore investigates the potential of soapstone rocks and the variation of TES performance of soapstone and granite rocks depending on their geological tectonic setting of origin so as to understand the impact of geo-tectonic settings to the site specificity in the TES potential of rocks.

1.3 Rationale of the Study

This study is taking a novel approach to investigate the patterns and nature of variabilities in the TES properties of rocks. By determining the variations depending on the geo-tectonic settings of rock origin, the study sets a precedence for similar studies. Thus, eventually creating databases as guidelines that can enable rock TES properties to be approximated, when precise data is not yet available onsite. Moreover, the research will provide benchmark information on the suitability of rock materials, found in some parts of Tanzania, for thermal energy storage application. It will also add to the body of knowledge on how suitability of rock materials varies with different rock types and within a specific rock type. Lastly, it will inform on the performance of soapstone rocks as thermal energy storage material.

1.4 Research Objectives

1.4.1 Main Objective

To experimentally investigate the variation in the potential of selected Tanzanian rocks (soapstone and granite) for their suitability in thermal energy storage for solar drying application and concentrated solar power generation.

1.4.2 Specific Objectives

- (i) To determine the thermo-physical, mechanical, and chemical properties of granite and

soapstone rocks as sensible thermal storage materials at solar drying and concentrated solar power temperatures.

- (ii) To investigate the variability in the thermal energy storage properties of granite and soapstone rocks depending on the geo-tectonic setting of origin.
- (iii) To compare thermal storage performance of granite and soapstone with other commonly used storage materials.

1.5 Research Questions

- (i) What are the thermo-physical, mechanical, and chemical properties of granite and soapstone rocks as sensible thermal storage materials at solar drying and concentrated solar power temperatures.?
- (ii) How is the variability in the thermal energy storage properties of granite and soapstone rocks depending on the geo-tectonic setting of origin?
- (iii) How is the thermal storage performance of selected natural rocks as compared to other commonly used storage materials such as molten salts?

1.6 Significance of the Study

This study will enable the local communities and industry to have information on the patterns and trends on the performance of rocks depending on their tectonic and geological settings. This will reduce the need to repeatedly perform characterisation due to the site specificity of the rocks (Adeleke & Airoboman, 2019). Since characterisation for rock thermal properties is very expensive determining the patterns in the thermal behavior of rocks will enable the selection of the rocks to be economical and affordable. And consequently, the utilization of rocks in thermal applications will increase. Hence making good use of this natural resource in increasing food security through solar drying for preservation and value addition (Kant *et al.*, 2016) and also powering off grid areas using CSP generation (Bouvry *et al.*, 2017).

1.7 Delineation of the Study

Despite Tanzania's abundance of rocks, this study will focus on granite and soapstone rocks both from the Craton and Usagaran geo-tectonic settings. This is because Craton geo-tectonic setting is the most stable and ancient cores of the continental crust while Usagaran is the oldest of all the Proterozoic mobile belts. Granite rocks are relevant in this study because they are the most abundant rocks globally and possess the highest variety in terms of structure and composition.

Soapstone rocks have been selected so as to investigate its potential in TES due to its excellent thermal properties and prevalence in most other thermal applications since ancient years.

CHAPTER TWO

LITERATURE REVIEW

2.1 Introduction

Solar thermal energy is a promising method for various applications including electricity generation and agricultural products drying. However, due to intermittent and unpredictable nature of solar radiation, solar thermal energy supply is unpredictable and diffused, necessitating the introduction of energy storage systems. Therefore, to have a solar power drying system or a power plant to function as a standalone system that does not require supplementary fuel and interoperability, thermal storage system (TES) is imperative.

2.2 Thermal Energy Storage

Although solar energy is abundant, clean and inexhaustible it has a challenge of intermittence (Eddemani *et al.*, 2021). The intermittency and unpredictability caused by the changes in the atmospheric conditions that lead to the weakening of solar irradiation, during which there is insufficient energy to run the required solar applications (Vindel & Polo, 2014). Moreover, the availability of solar energy is also time dependent thus creating an energy gap between supply and demand (Singh *et al.*, 2010; Suresh & Saini, 2020). The integrated of thermal energy storage (TES) system can mitigate the impacts of the intermittent nature of solar radiation (Bal *et al.*, 2011; Kant *et al.*, 2016; Muh & Tabet, 2019). The TES systems maximizes solar thermal energy and ensure a prolonged energy availability (Suresh & Saini, 2020) by storing excess thermal energy that may have been wasted and provide it for use when the solar radiation is insufficient (Bataineh & Gharaibeh, 2018).

2.3 Materials Used for Thermal Energy Storage

A suitable material for TES should have high energy density, which is a function of specific heat capacity and density, and high thermal conductivity (Adeleke & Airoboman, 2019; Kant *et al.*, 2016). High thermal capacity is desirable to reduce the required storage volume and containment structure costs. Thermal conductivity of the materials should be high enough to allow sufficient heat transfer in a small temperature gradient (Navarro *et al.*, 2012). The compressive strength of the material should be high in order to prevent the crushing of the bottom layers of the rocks from crushing due to the weight of the rocks above it. It should also have high chemical stability at high temperature (Srivastava *et al.*, 2020).

2.3.1 Common TES Materials

Materials studied for thermal energy storage application are divided into four families namely ceramics and glasses, metals and alloys, polymers and elastomers and hybrids include salts, aluminum beads, ceramic materials and rocks (Alva *et al.*, 2017). The most common TES materials and highlights on their strengths and weaknesses for thermal energy storage applications are as summarized in Table 1. Whereby most materials showed strengths as TES materials with high maximum service temperature. However, the most common weakness as TES materials was the high cost of investment. Materials with high cost of investment include reinforced concrete, castable ceramic, alumina ceramics, silicon carbide ceramics, copper, iron-cast iron, lead, cofalit, mineral oil and synthetic oil. Additionally, most low-cost materials such as bricks, cement mortars, concrete and sand had low thermal capacity and/or low thermal conductivities.

However, sufficient thermal capacity of the TES material lowers the material containment volume and as a result may assist in subsidizing the investment costs (El Alami *et al.*, 2020). Materials with suitable thermal capacity include alumina ceramics, Brick magnesia, copper, cast iron, cofalit, molten salts, water and demolition wastes. To ensure that the TES system has proper charging and discharging rates the TES material needs to have good thermal conductivity (Tiskatine *et al.*, 2017). Materials with good thermal conductivities include alumina ceramics, silicon carbide ceramics, brick magnesia, copper, cast iron, aluminium, lead, cofalit, graphite, sodium chloride and liquid sodium.

Table 1: Common materials used for thermal energy storage and their limitations

Material	Strengths	Limitations	References
Concrete	Easy and cheap to manufacture	Inadequate tensile strength and thermal conductivity	Wang et al. (2020)
HT concrete	Low cost, high compressive and tensile strength	Inadequate thermal conductivity	Cabeza et al. (2015); Laing et al. (2006)
High alumina concrete	High maximum service temperature	Inadequate thermal conductivity	Tiskatine et al. (2017)
Reinforced concrete	Low cost of materials and processing	Costly and difficulty in machining	Tiskatine et al. (2017)
Cement mortar	Low cost of materials and processing	Inadequate thermal energy density and conductivity	Koçak et al. (2020); Tiskatine et al. (2017)
Castable ceramic		Excessive cost of investment	Cabeza et al. (2015)
Alumina ceramics	High thermal capacity and conductivity	Costly and difficulty in processing	Tiskatine et al. (2017)
Silicon carbide ceramics	High thermal conductivity	Poor thermal shock resistance, Costly and difficulty in processing	Tiskatine et al. (2017)
Brick	Low cost material	Inadequate thermal energy density and low maximum operating temperature	Tatsidjodoung et al. (2013)
Brick magnesia	High maximum service temperature	Poor thermal shock resistance	Herrmann and Kearney (2002)
Silica fire bricks	Medium high maximum service temperature	Inadequate mechanical strength	Herrmann and Kearney (2002)
Copper	High maximum service temperature	Excessive cost of investment and thermal expansion	Suresh and Saini (2020)
Iron-cast iron	High thermal capacity and conductivity	Excessive cost of investment, unit weight and thermal expansion	Herrmann and Kearney (2002)
Aluminium	High maximum service temperature and thermal conductivity	Excessive thermal expansion	Suresh and Saini (2020)
Lead	High maximum service temperature and thermal conductivity	Excessive cost and inadequate thermal capacity	Suresh and Saini (2020)
Cofalit	High maximum service temperature and thermal	Costly and difficulty in production	Koçak et al. (2021)

Material	Strengths	Limitations	References
	capacity		
Graphite	High maximum service temperature	At higher temperature it reacts with air to form CO ₂	Price et al. (2002)
Sodium chloride	High thermal capacity	Excessive thermal expansivity	Alva et al. (2017)
Molten salts	High thermal capacity	Inadequate thermal conductivity, excessive cost of investment and freezing temperature, very corrosive	Alva et al. (2017)
Solar salt	Versatile (as sensible and phase change TES material)	Inadequate thermal conductivity, corrosive	Caraballo et al. (2021)
Mineral oil	Does not require heat exchanger	Inadequate thermal conductivity, excessive cost of material	Alva et al. (2017)
Synthetic oil	Non-corrosive to plant components	Inadequate thermal conductivity and lifespan, excessive cost of investment	Fasquelle et al. (2017)
Liquid sodium	High conductivity	Dangerously excessive vapour pressure	Herrmann and Kearney (2002)
Water	High thermal capacity	Inadequate conductivity, excessive vapour pressure and corrosiveness when used as steam	Wang et al. (2020)
Demolition wastes	High thermal capacity, waste to resource conversion	Inadequate thermal conductivity	Koçak et al. (2020)
Sand	Cheap and readily available	Inadequate energy density and thermal conductivity	Suresh and Saini (2020)

2.3.2 Natural Rocks

Rocks are TES materials that have been studied to offer the potential of low cost because of their abundance and affordability (Adeleke & Airopoman, 2019). The majority of studies on rocks as thermal energy storage materials focused on packed beds and rock pebbles (Adeleke & Airopoman, 2019). Some of the most commonly used rocks for TES are granite, limestone, marble, quartzite, sandstone, granodiorite, gabbro, basalt, hornfels, schist, quartzitic sandstone, rhyolite, andesite, calcareous sandstone, steatite/soapstone, dolerite, gneiss, diorite and dolomite rocks (Eddemani *et al.*, 2021; Tiskatine *et al.*, 2017).

2.4 Rocks Variations in Geo-Tectonic Settings

Rock variability is caused by factors such as disjointedness conditions, characteristics of the formative materials, eon and weathering and climatic conditions (Aladejare & Wang, 2016), these factors are also dependent on geological tectonic settings (Valentine & Connor, 2015; Veizer &

Mackenzie, 2014). Tanzania's crust has evolved through complex tectonic movements leading to its specific geological setting and abundance of minerals (Lemenkova, 2022). Tanzania has two main geotectonic settings; the Archean Tanzanian Craton and the Proterozoic mobile zones (Begg *et al.*, 2009; GST, 2015). Mobile belts are metamorphic belts with younger rocks that have more length than breadth and are destined to attain cratonisation as their final stage so as to become cratons (Tankard *et al.*, 2012).

2.4.1 Archean Craton Geo-Tectonic Setting

Cratons are the most stable and ancient cores of the continental crust formed in the 2.5-4.0 giga-annum (Ga) mostly during the Archean eon (James & Fouch, 2002; Sawada *et al.*, 2018). In Africa, the Archean cratons were formed around 3.6-2.5 Ga and includes the West African, Congo, Ugandan, Maltahohe, Kalahari, Enigmatic and the Tanzanian cratons (Begg *et al.*, 2009; Micallef, 2019). The Tanzanian Craton is comprised of The Kavirondian, Nyanzian and Dodoma supergroups, the later supergroup being the basement containing the oldest rocks (Godfray *et al.*, 2022; Kabete *et al.*, 2012). The Dodoma supergroup chronology of formation includes sedimentation in 3.6 mega-annum (Ma) followed by volcanic action in 2.8 Ma and metamorphism continued in later years (Kabete *et al.*, 2012; Sun *et al.*, 2018). It is comprised of granitoids including granite rocks accompanied by high and low grade metamorphic rocks including soapstone (Sun *et al.*, 2018).

2.4.2 Proterozoic Geo-Tectonic Setting

The Proterozoic geo-tectonic setting is a mobile belt as opposed to the stationery craton belt (Banerjee, 2020; Begg *et al.*, 2009). It is divided into three types; the Palaeoproterozoic mobile belts comprising of Usagaran and Ubendian; Mesoproterozoic mobile belt of Karagwe-Ankolean and; the Neoproterozoic mobile belts of Mozambique and the Malagarasi supergroup (GST, 2015). Being a Palaeoproterozoic, the Usagaran is the oldest belt of all the types of the Tanzanian Proterozoic geotectonic belts (Fritz *et al.*, 2005; Mori *et al.*, 2018) and is found on the Southeastern margin of the Craton (Sommer & Kröner, 2013) as shown in Fig. 1. The rocks in Usagaran mobile belt has a combination of mafic, pelitic sedimentary and marine carbonates (Godfray *et al.*, 2022; Moeller *et al.*, 1995).

2.5 Characterization Parameters

2.5.1 Thermo-Physical Properties

(i) Thermal Capacity

It is the product of the density and specific heat capacity of rocks and it increases when heated. Specific heat capacity usually increase with temperature until it reaches a nearly constant value (El Alami *et al.*, 2020). This is due to the increase in the rotational and translational energy of the molecules until they reach a constant value. On the other hand, the changes in the density with heating is almost negligible hence, assumed to be constant (Wang *et al.*, 2020). Generally it is desirable that not only density but also specific heat capacity parameters to be high so that thermal capacity leading to enhanced stored thermal energy (Kant *et al.*, 2016).

(ii) Thermal Conductivity and Thermal Diffusivity

It is the capacity of a material to allow heat transfer or diffusion thus controlling the rate at which the heat can therefore be released or extracted, thermal conductivity is one of the important parameters to consider in the determination of the suitability of a material for TES application (Jones, 2003; Tiskatine *et al.*, 2017). It gives a clue of how easy or difficult a material allows flow of thermal energy from the outer surface into the interior (Adeleke & Airoboman, 2019; Kant *et al.*, 2016). Thermal conductivity of crystalline rocks has been observed to decrease as opposed to amorphous rocks whose thermal conductivities increase with the increase in temperature (Nahhas *et al.*, 2019).

(iii) Porosity

Porosity represents the fraction of the void spaces in a solid material such as a rock and affects thermal conductivity, which in turn determines the suitability of a material/rock for TES. High porosity leads to reduced bulk density, thermal conductivity and compressive strength (Jones, 2003; Shang *et al.*, 2019). It is therefore important to consider porosity when selecting rocks suitable as thermal energy storage materials to be applied in CSP plant (El Alami *et al.*, 2020).

2.5.2 Thermo-Mechanical Properties

Mechanical properties, especially young modulus, are critical when it comes to material suitability for thermal energy storage application since it can determine the hardness and uni-axial strength of the material (Li *et al.*, 2019). Having higher compressive strength will enable the rock bed bottom layers to withstand crushing despite the weight of the rocks above it (Adeleke &

Airoboman, 2019; Kant *et al.*, 2016). The mechanical properties are important since they also influence the thermal conductivity and diffusivity of crystalline rocks (El Alami *et al.*, 2020).

2.5.3 Thermo-Chemical Properties

The mineralogical and chemical compositions of rocks influence their thermal stability significantly (Shang *et al.*, 2019). They help to predict various chemical reactions which may occur with temperature increase. Furthermore, they enable the minimum and maximum operating temperatures of the rocks to be defined (El Alami *et al.*, 2020).

2.6 Selected Work on Rocks as TES Materials

As the widest spread rocks in the crust continental crust that come in a variety of properties including chemical composition and grain sizes (Allen *et al.*, 2014; Haldar & Tišljär, 2014) granites are also expected to be the most widespread rocks across a diverse range of geo-tectonic settings. A variety of studies have shown a considerable difference in the properties of granite. In his study, Shang *et al.* (2019) studied fine to medium grained granite rocks from China. Experiments performed include the X-ray diffraction (XRD), the Mercury intrusion porosimetry (MIP), the P-wave velocity and the uniaxial compressive test at temperatures from 25°C to 1200°C. These experiments intended to deduce the mineral composition, maximum diffraction intensity, pore structure, p-wave velocity, and uniaxial compressive stress and strain, respectively. The experimentation showed that the granite samples had only non-hydrothermal minerals such as feldspar, quartz, pyroxene and illite. Hence, the study showed that granite rocks are potential TES materials in systems of up to 800°C.

On the contrary, Grirate *et al.* (2014) studied granite samples from Morocco and found them composed with the hydrothermal mica. The study measured the rock geochemistry and mineralogical composition, porosity, uniaxial compressive strength, thermal decomposition and thermal capacity. To obtain the above-mentioned properties, the samples underwent through the petrographic examination, the hydrochloric acid test and the compressive strength test at room temperature. Additionally, the X-ray Fluorescence spectrometry (XRF), the Thermogravimetric analysis (TGA) and the differential scanning calorimetry (DSC) were conducted at a temperature range from 25°C to 400°C.

Similarly, granite rocks studied by Li *et al.* (2019) had the hydrothermal mica detected using the X-ray diffraction (XRD) technique. In the study performed by Alzahrani *et al.* (2022), the petrographic examination, the thermo-gravimetric analysis, the double beam spectrophotometer, the dilatometer, the XRF, the XRD, and the DSC techniques were conducted. Data on chemical

composition, porosity, bulk density, compressive strength, abrasion resistance, thermal decomposition, linear thermal expansion and spectral reflectance were obtained from the characterisation. It was consequently noted that there was a variety in the mineral composition of the studied eight granite samples where only two had the hydrothermal mica (biotite, muscovite and annite), five samples had the alteration minerals (zeolite, prehnite, kaolinite) and three of the eight samples had neither of the two thermally unstable groups of minerals.

Soapstone rocks have a very high thermal shock resistance than majority of natural rocks (Huhta *et al.*, 2016) and has been used since ancient times for internal linings of stoves and fire chambers making cooking pots, metal casting molds, high temperature electrical components and cladding for various types of stoves (Kora, 2020) but has not been studied for use as a thermal energy storage material. Huhta *et al.* (2019) studied the composition and structure of magnesite soapstone in fire chambers construction by conducting the petrographic examination and the XRD experiments. It was observed that, the durability of the rock increased with further exposure in fire due to the formation of periclase mineral. A review study on the traditional soapstone as a cookware and culinary material by Kora (2020) shows that various studies reported that soapstone rocks have excellent thermal properties including high specific heat capacity, high density, high thermal resistance and are resistant to acid and alkali.

The aforesaid are a results of a diverse experimental characterization techniques including inductively the coupled plasma mass spectrometry (ICP-MS), the inductively coupled plasma optical emission spectroscopy (ICP-OES), the inductively coupled plasma mass spectrometry (ICP-MS) and the laser ablation time of flight inductively coupled plasma mass spectrometry (LA-TOF-ICP-MS). Other experiments conducted were the laser ablation inductively coupled plasma mass spectrometry (LA-ICP-MS), the neutron activation analysis (INAA), the particle induced gamma ray emission (PIGE) and the particle induced X-ray emission (PIXE). Additionally, the Mössbauer spectroscopy, the atomic absorption spectrophotometry (AAS), the energy dispersive energy-dispersive X-ray fluorescence (ED-XRF) were conducted. The study also mentions the XRD, the TGA and the optical microscopy as relevant experiments that led to the aforementioned findings. Lastly, the visible near infrared reflectance spectrometry, the Fourier transform infra-red spectroscopy (FTIR), the scanning electron microscopy (SEM), the Brunauer-Emmett-Teller (BET) surface area, the Raman spectroscopy and the petrography experiments were also conducted. Due to these afore-mentioned excellent thermal properties it is relevant to investigate soapstone rocks' potential as TES materials.

Additionally, even rocks of a particular type may exhibit different properties depending on their mineralogical variations, thus potentially affecting their suitability for energy storage application

(Adeleke & Airoboman, 2019; El Alami *et al.*, 2020). Nahhas *et al.* (2019) conducted experimental characterization on basalt rocks from France and Egypt. Experiments included scanning electron microscope with energy dispersive spectroscopy (SEM-EDS), XRD, DSC, laser flash apparatus (LFA), pushrod dilatometer, and high-temperature ultrasonic technique. Findings of the two rocks showed a variation in the thermal energy storage potential whereby, the basalt from France had in terms of chemical and mineralogical stability, thermal expansion, structural analysis, thermal conductivity and thermal capacity as opposed to the basalt from Egypt. Additionally, thermal cycling tests, thermo-physical and mechanical experiments conducted on rhyolite rock concluded that the thermal energy storage parameters vary in a rock of a similar type (Tiskatine *et al.*, 2017).

Moreover, the study on primitive basalt rocks from Spain and France could perform well as thermal energy storage materials and had more stable thermal properties as opposed to the evolved basalts from Egypt and Greece (Bouvry *et al.*, 2017). These findings were deduced using XRF, DSC, SEM, drop calorimetry, infrared spectroscopy, LFA and XRD characterisation techniques. The experiments aimed to derive the chemical and mineralogical composition, thermal capacity, calorific capacity, thermal diffusivity, thermal conductivity, thermal expansion, melting temperatures and infrared emissivity. Since most of these few researches on the suitability of specific rock types for TES were conducted in the developed countries, and given site specificity and variation of the properties even same rock type (Adeleke & Airoboman, 2019; Alva *et al.*, 2017; El Alami *et al.*, 2020), there is a need to conduct such investigations in Africa, particular sub-Saharan Africa where energy problem is contributing to underdevelopment and non-industrialization.

CHAPTER THREE

MATERIALS AND METHODS

3.1 Introduction

The study aims to experimentally investigate the variability in the potential of selected natural rocks as TES materials for concentrated solar generation and solar drying applications. The variability is tested across the main two types of geo-tectonic settings in Tanzania and selecting the most ancient category of supergroups in each. Rock samples were collected, prepared and experimented in the lab. Experimental characterization of selected natural rocks (soapstone and granite) was done to investigate the thermo-chemical, thermo-physical and thermo-mechanical properties of the rocks at 20-950°C.

3.2 Materials

The rock samples were obtained in Tanzania from two geo-tectonic settings of Craton and Usagaran as shown in Table 1. Tanzania has two main geotectonic settings; the Archean Tanzanian Craton and the Proterozoic mobile zones (Begg *et al.*, 2009; GST, 2015). The most ancient rocks in the craton are found in the Dodoma Supergroup in Dodoma region (Godfray *et al.*, 2022) while, the most ancient Proterozoic rocks were found in Usagaran mobile belt in Iringa region (Mori *et al.*, 2018). Granite rocks are the most widespread in the continental crust with the largest recorded rock variations especially in terms of chemical composition and structure (Halder & Tišljär, 2014). Hence, they were selected so as to study the variability in their potential as TES material. Soapstone rocks were also selected so as to study their potential and variability as a TES material.

Soapstone has been mentioned to have high thermal shock resistance (Huhta *et al.*, 2016) and excellent thermal properties (Kora, 2020). As such it has been used since ancient years for various thermal application including cooking utensils (Frink *et al.*, 2012), internal lining of ovens, fireplaces and stoves (Huhta *et al.*, 2019; Pirinen, 2005) and in high temperature components of electrical and electronic appliances (Kora, 2020). Therefore, the rocks from Craton geotectonic setting were obtained from Dodoma and those from Usagaran were collected from Iringa region as shown in Fig. 1. The soapstone from Craton and Usagaran were coded CS and US respectively and the granite from Craton and Usagaran are coded CG and UG respectively as shown in Table 2.

Table 2: Sample code names according to geo-tectonic setting and rock type

ROCK TYPE	GEO-TECTONIC SETTING	SAMPLE CODE
Soapstone	Craton	CS
	Usagaran	US
Granite	Craton	CG
	Usagaran	UG

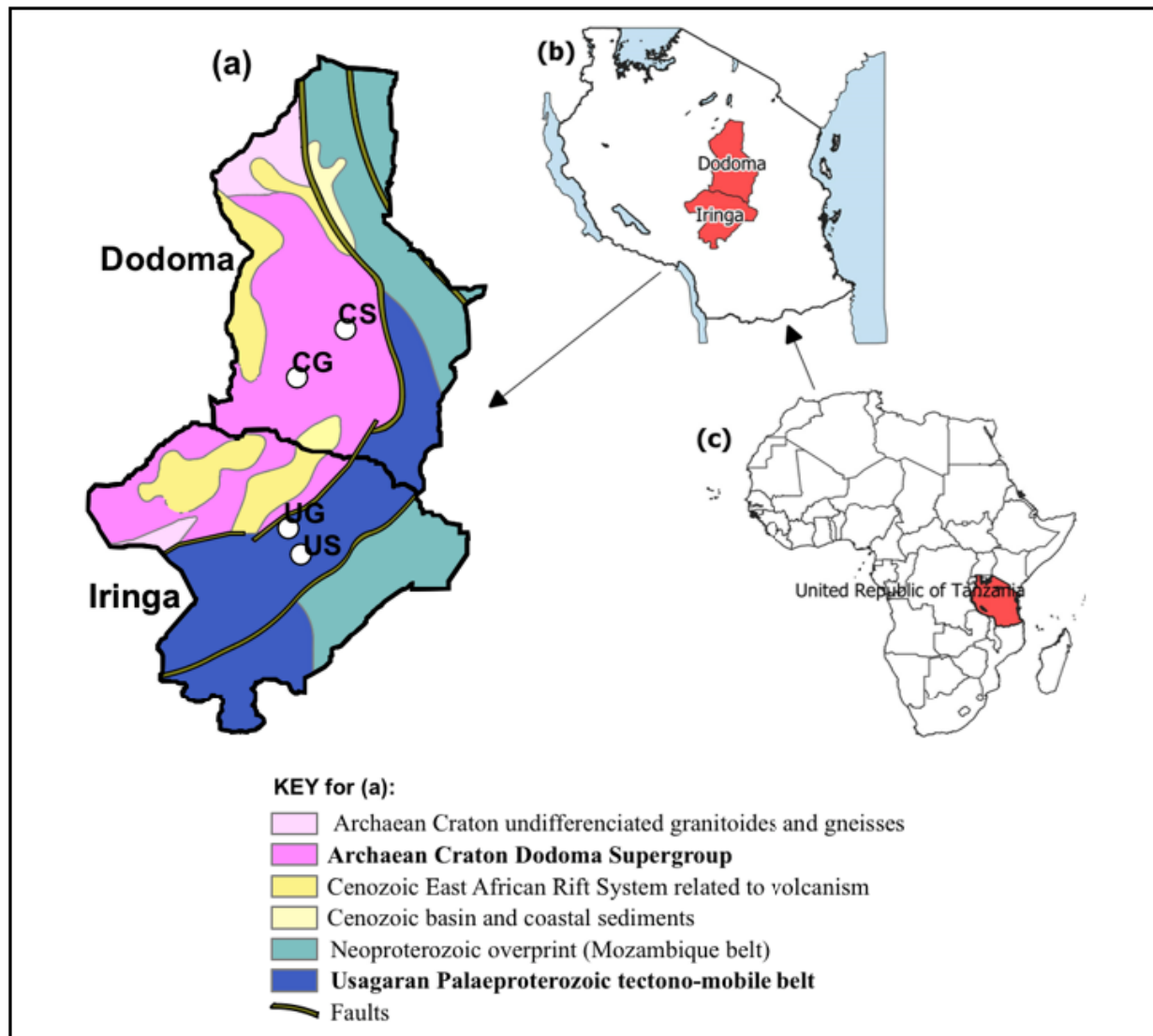


Figure 1: Map showing the location of the collected rock samples (a) Map of Dodoma and Iringa regions showing sample collection locations and their geo-tectonic settings (b) Map of Tanzania showing the locations of Dodoma and Iringa regions (c) Map of Africa showing the location of Tanzania

3.3 Characterisation of Rock Samples

Experimental investigation through rock characterisation was done so as to study their properties as TES materials. The characterization experiments on the thermo-physical, thermo-chemical and thermo-mechanical properties as related to thermal energy storage were done as summarized in Fig. 3. The characterization was done for low temperatures less than 150°C (Wang *et al.*, 2020) to

examine the solar drying applications potential (Kant *et al.*, 2016) and higher temperatures greater than 300°C (Hrifech *et al.*, 2019) to examine the concentrated solar power generation potential (Tiskatine *et al.*, 2017) of the rock materials. The rocks were prepared into powder, square and cubical sample sizes for experimentations as shown in Fig. 2.

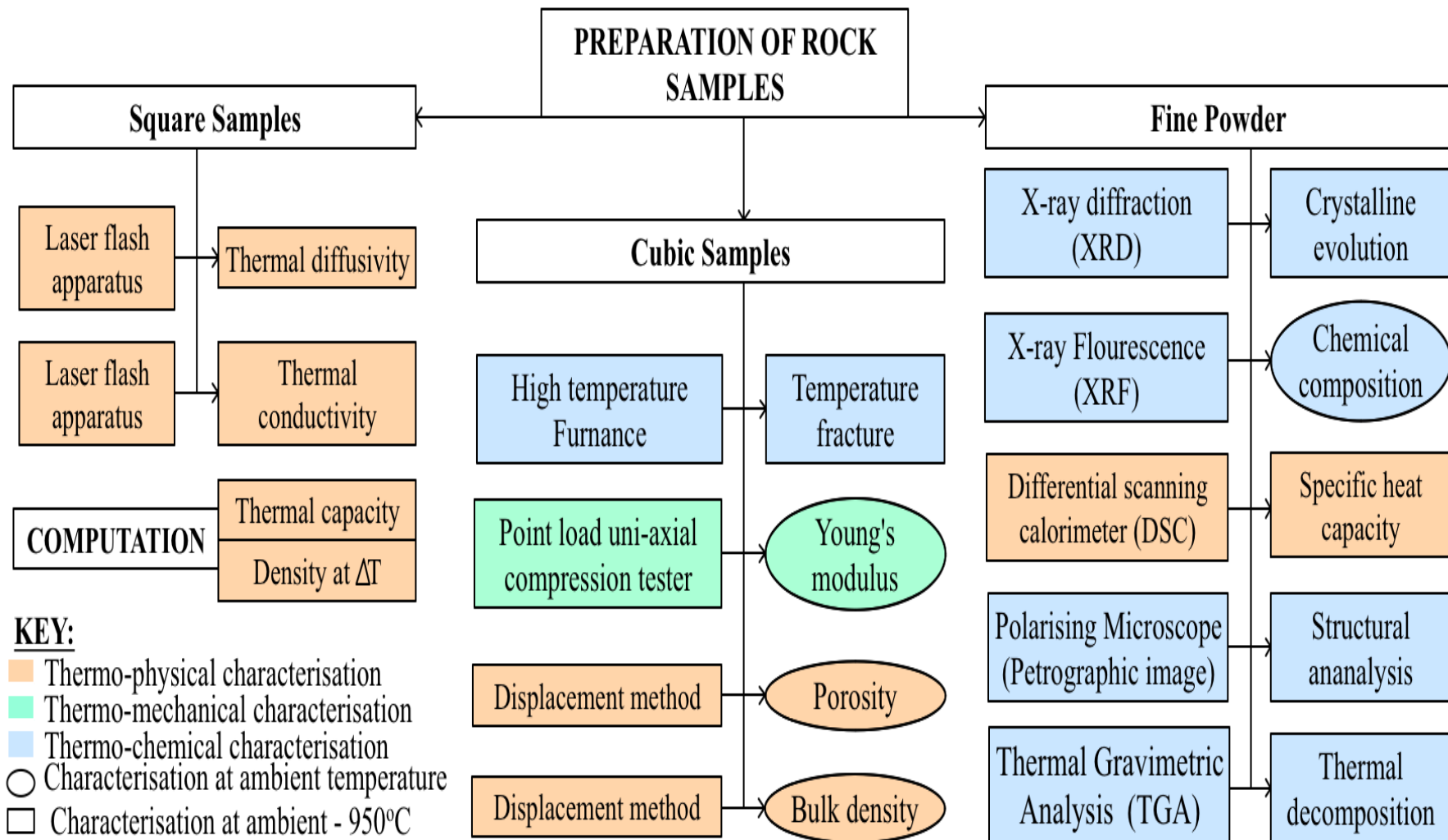


Figure 2: The characterization experiments for thermal energy storage

3.3.1 Thermo-Chemical Properties

Thermal stability was determined using the thermal gravimetric analyzer (TGA); crystalline phases were studied using the X-ray diffraction (XRD); structural analysis was studied through the petrographic imaging. Moreover, chemical composition was determined using the X-ray fluorescence (XRF) and; high temperature test was done in the high temperature furnace. The experiments will eventually enable us to deduce the chemical stability and thermal shock resistance at elevated temperatures.

(i) Chemical Composition

X-ray Fluorescence technique was used to measure the oxides and elemental composition of the rocks for predicting the chemical reactions at higher temperatures and mechanical stability of the rocks (Srivastava *et al.*, 2020). The XRF method was selected because it is not only a matured and most common methodology in geochemistry but also, possess spectrum of clear emissions that ensures a precise and accurate data (Oyedotun, 2018). Whereby, 1 g of pressed powder pellets of the rock samples were used in the Bruker AXS S4 spectrometer in the presence of P10 detector gas.

(ii) Structural Analysis

Petrographic examination was performed in order to identify the rock types and to determine structure of the rocks including the rocks mineralogy, grain size and foliation of the rock specimens (Nahhas *et al.*, 2019). The rocks were cut into slices, mounted on a glass slide, and ground to the standard thin section thickness of 0.03 mm for the examination of optically transparent minerals. The petrographic characterization of the prepared specimens was achieved using a Carl Zeiss Primotech polarizing microscope equipped with built-in camera. The acquisition and manipulation of the micrographs were undertaken by the aid of MATSCOPE software.

(iii) Crystalline Phases

The Crystalline evolution was measured so as to determine the available phases and predict the reactions in the rock at higher temperatures (Nahhas *et al.*, 2019). Bruker D8 ADVANCE X-ray diffractometer equipment was used to measure powdered samples of 150 μm . The equipment was fed with a primary Ge_{111} monochromator, a LinxEye silicon strip detector and a current of wavelength 1.54059 Å from a Cu-tube. The samples were measured in the range 2° to 90° 2θ , at steps of 0.02° and a rate of 4 s per step.

(iv) Thermal Decomposition

The thermo-gravimetric analysis was performed for deducing the thermal stability and the volatility of the rocks' constituting materials with temperature increase (Alzahrani *et al.*, 2022) . About 3.5 ± 0.3 mg of $<63 \mu\text{m}$ powdered sample was used in the TG/DTA 6300 machine. The process took place from 40°C to 950°C at the rate of $10^\circ\text{C}/\text{min}$. Alumina (Al_2O_3) was used as a reference material.

(v) High Temperature Test

High temperature test to observe the capacity of the rocks to resist fracture caused by increase in temperature up to higher temperatures (Abdollahnejad *et al.*, 2020). Samples of $10 \times 10 \times 10$ mm were enclosed in a CBFL518C Cole Palmer Box furnace and exposed to 700°C and 1000°C (Nahhas *et al.*, 2019) for 6 hours, these number of hours enables the rock samples to reach a steady temperature field (Chen *et al.*, 2021). They were left to gradually cool in the furnace until they reached room temperature (Abdollahnejad *et al.*, 2020).

3.3.2 Thermo-Physical Properties

The thermo-physical properties included density and porosity studied using the displacement method; specific and thermal capacity experimented using the differential scanning calorimetry (DSC) and; thermal diffusivity and conductivities determined through the laser flash apparatus (LFA). These experiments will study the energy density and the expected charging and discharging rates of the rocks.

(i) Specific and Thermal Capacity

The evolution of specific heat capacity from 20 - 950°C was measured so as to compare the expected amount of heat stored in a unit mass (Bal *et al.*, 2010). Powder samples of $150 \mu\text{m}$ were used in NETZSCH DSC 404 F1 Pegasus differential scanning calorimeter against sapphire as calibration standard. Heating was done under air atmosphere at rate of $10^\circ\text{C}/\text{min}$. First the measurement for the baseline and the standard was done over the temperature range. Followed by measuring the sample and then the standard ratio method was used to compute the specific heat capacity (Hartlieb *et al.*, 2016). Thermal capacity was calculated as a product of density and specific heat capacity as shown in Equation 1.

$$\text{Thermal capacity at temperature } T \left(C(T) \right) = \left(C_p(T) \right) \times \left(\rho(T) \right) \quad (1)$$

(ii) Thermal diffusivity and conductivity

Additionally, a laser flash apparatus was used to determine the thermal diffusivity and thermal conductivity so as to understand the rates of thermal charging and discharging of the rock samples (Bal *et al.*, 2010; El Alami *et al.*, 2020). Samples of 10 x 10x 1.5 mm were placed on a graphite holder in the NETZSCH LFA 427 Micro-flash apparatus under argon atmosphere and vacuum of 10^{-2} mBar. Heating was then done at a rate of 2.5°C/min from ambient temperature to 950°C.

(iii) Bulk density

Densities (ρ) of the four rock types was determined so as to compare the expected containment volumes of the rocks in relation to amount of heat stored (Bal *et al.*, 2010). The experimentation was conducted according to the standard procedure of ASTM C128-15 by American Society for Testing and Materials ASTM (2013) for Relative Density of Fine Aggregates. For each experiment, rock sample cubes of 10 x 10 x 10 mm³ were weighed by an analytical balance to get mass W in grams. They were kept in the measuring cylinder and 50 cm³ of water was added until the cylinder reached volume V in cm³. The density at room temperature was then calculated using Equation 2.

$$\text{Density } (\rho) = \frac{W}{V - 50} \quad (2)$$

Densities at higher temperatures ($\rho(T)$) were calculated from thermal conductivity ($\lambda(T)$) thermal diffusivity ($\alpha(T)$) and specific heat capacity ($C_p(T)$) at that temperature (Nahhas *et al.*, 2019) using Equation 3.

$$\text{Density at temperature T } (\rho(T)) = \frac{(\lambda(T))}{(C_p(T)) \times (\alpha(T))} \quad (3)$$

(iv) Relative Porosity

Rock porosity was obtained so as to determine the amount of air spaces in the rock samples as they tend to affect conductance and mechanical properties of the rocks (Kant *et al.*, 2016; Rybacki *et al.*, 2015) by following the ASTM C128-15 standard procedure for Absorption of Fine Aggregate (ASTM, 2013). For each experiment, rock sample cubes of 10 x 10 x 10 mm³ were weighed by an analytical balance to get mass W in grams. They were consequently soaked in the water for 72 \pm 4 h while stirring every 24 h and then surface dried and weighed to get mass M. The porosities were deducted by using Equation 4.

$$\text{Porosity} = \frac{(M - W) \times \rho_{rock}}{W \times \rho_{water}} \dots\dots\dots (4)$$

3.3.3 Thermo-Mechanical Properties

The thermo-mechanical properties studied were the Young’s modulus obtained using the nano-indentation method.

(i) Young’s modulus

The Young’s modulus was determined so as to deduce the ability of the lower layer of rocks to withstand the loading from upper layer of rocks. Nano-indentation instrumentation method was used because rocks are heterogenous materials and its useful to get the average mechanical strength as a function of their heterogeneity (Borodich *et al.*, 2015; Ma *et al.*, 2020). Polished cylindrical samples of 5 mm diameter and 20 µm thickness were used in Nanoindentation Tester NHT³ machine with a Berkovich indenter. The experiment was done following the method by Oliver and Pharr (2011) with the maximum loading of 200 Mn at a loading and unloading rate of 600 Mn/min and a Poisson’s ratio of 0.3.

CHAPTER FOUR

RESULTS AND DISCUSSION

4.1 Overview

For thermo-chemical properties, results including thermal stability, crystalline phases, structural analysis, chemical composition and high temperature are discussed. The discussion also encompasses the thermo-physical properties results for density and porosity, specific and thermal capacity and, thermal diffusivity and conductivities. Lastly are the Young's modulus results to discuss the thermo-mechanical properties. Of all the four experimented rocks, the soapstone rock from the Craton geo-tectonic setting (CS rock) had the most desired properties for thermal energy storage.

4.2 Thermo-Chemical Properties

4.2.1 Chemical Composition

Chemical composition in terms of oxide percentages was obtained using the XRF technique and are shown in Fig. 3. In soapstone samples, the main elements are Silicon dioxide and Magnesium oxide. Their dominance in the composition is caused by the domination of talc a mineral with hydrated magnesium silicate i.e. $\text{Mg}_3\text{Si}_4\text{O}_{10}(\text{OH})_2$ amounting to values greater than 90%, (Baron *et al.*, 2016; Strecker *et al.*, 2010). The most dominant elements in granite samples are Silicon dioxide and aluminum oxide also resembling the findings in Srivastava *et al.* (2020). Maqsood *et al.* (2004) explains that when the SiO_2 content greater than 65% of the oxide's composition of an igneous rock it verifies that the rock is a granite rock. Hence, the igneous rocks UG and CG fall in the granite rocks group because their SiO_2 content is approximately 70%. The granite rocks are peraluminous since Al_2O_3 content is greater than the summation of Na_2O , K_2O and CaO , as explained in Srivastava *et al.* (2020). Sun *et al.* (2018) also reports on the presence of peraluminous granite in the Tanzania craton. Bouvry *et al.* (2017) observed that high amounts of silicon oxides contribute to higher strength properties.

Furthermore, Nahhas *et al.* (2019) explains that high amounts of hematite contribute to crystallization and wide temperature range stability of the rock. The soapstone rock CS has a significant amount of Fe_2O_3 amounting to 9.65 which is higher by 7.7% as compared to US rock. Variations in hematite levels occur in soapstone rocks while most granite rocks have low Fe_2O_3 (Shang *et al.*, 2019). Figure 3 and Table 3 shows that CS has higher amounts of Iron oxide, Nickel and Chromium as compared to US rocks, indicating that CS is an ultramafic soapstone while US

is a carbonate soapstone (Baron *et al.*, 2016). The carbonates in the carbonate soapstone rocks undergo chemical disintegration to form carbon dioxide at higher temperatures of $300^{\circ}\text{C} \leq t \leq 500^{\circ}\text{C}$ (Srinivasan *et al.*, 2020; Yavuz *et al.*, 2010). The carbonate nature the metamorphic rocks in Usagaran belt are due to the presence of marine carbonates deposited in the belt area (Moeller *et al.*, 1995). Also the carbonate soapstone rocks are found in zones with high tectonic activities and deformation (Baron *et al.*, 2016), a typical of the Usagaran belt as it is interrupted by tectonic faults as shown in Fig. 1. Therefore, chemical compositions of all granite and soapstone rocks show a promising mechanical strength, while that of CS shows higher potential of chemical stability because of its sufficient hematite content.

Table 3: Elemental composition of soapstone rocks

Wt.%	Ba	S	Mn	Cr	Zr	Co	Zn	Mo	Pb	Ni	Cu
CS	71	1021	319	719	8	307	61	2	3	1114	90
US	53	716	32	110	64	16	11	3	3	46	24

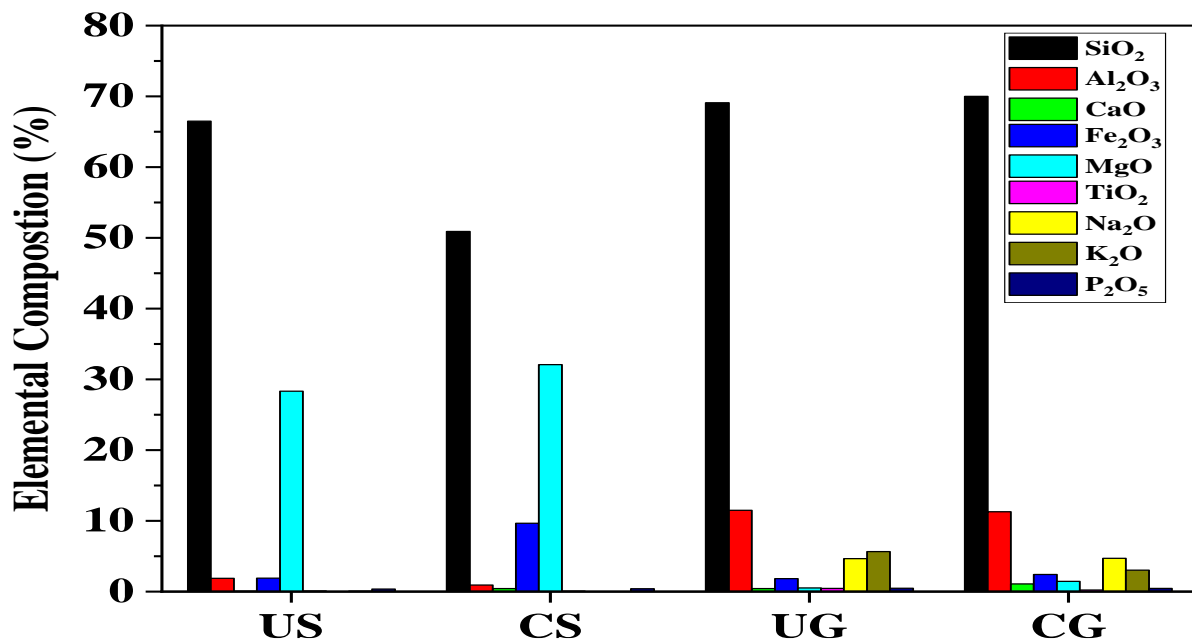


Figure 3: Graph showing Chemical composition of US, CS, UG and CG rocks

4.2.2 Crystalline Phases

This experiment determines the available phases essential in predicting the reactions in the rock at higher temperatures (Nahhas *et al.*, 2019). The XRD images in Fig. 4 (a) and (b) shows the constituents of granite rock samples. The granite UG has peaks representing quartz (SiO₂), albite (NaAlSi₃O₈), chlorite [(Mg,Fe,Al)₆ (Si,Al)₄O₁₀(OH)₈], magnetite (Fe₃O₄) and microcline (KAlSi₃O₈). These minerals correspond to the microcline-rich undeformed granite rocks that are found in the Usagaran belt (Manya & Maboko, 2016). The rock sample CG has peaks of quartz, Albite, Biotite [K(Mg,Fe)₃(AlSi₃O₁₀)(F,OH)₂], magnetite, Anorthite (CaAl₂Si₂O₈) and

Muscovite/mica $[KAl_2(AlSi_3O_{10})(FOH)_2]$. Muscovite and biotite are hydrothermal compounds and are thus susceptible to dehydration (El Alami *et al.*, 2020), causing the CG rock to be unstable at elevated temperatures. Biotite was marked to be common in the magmatic rocks of the Dodoma supergroup Craton (Sun *et al.*, 2018).

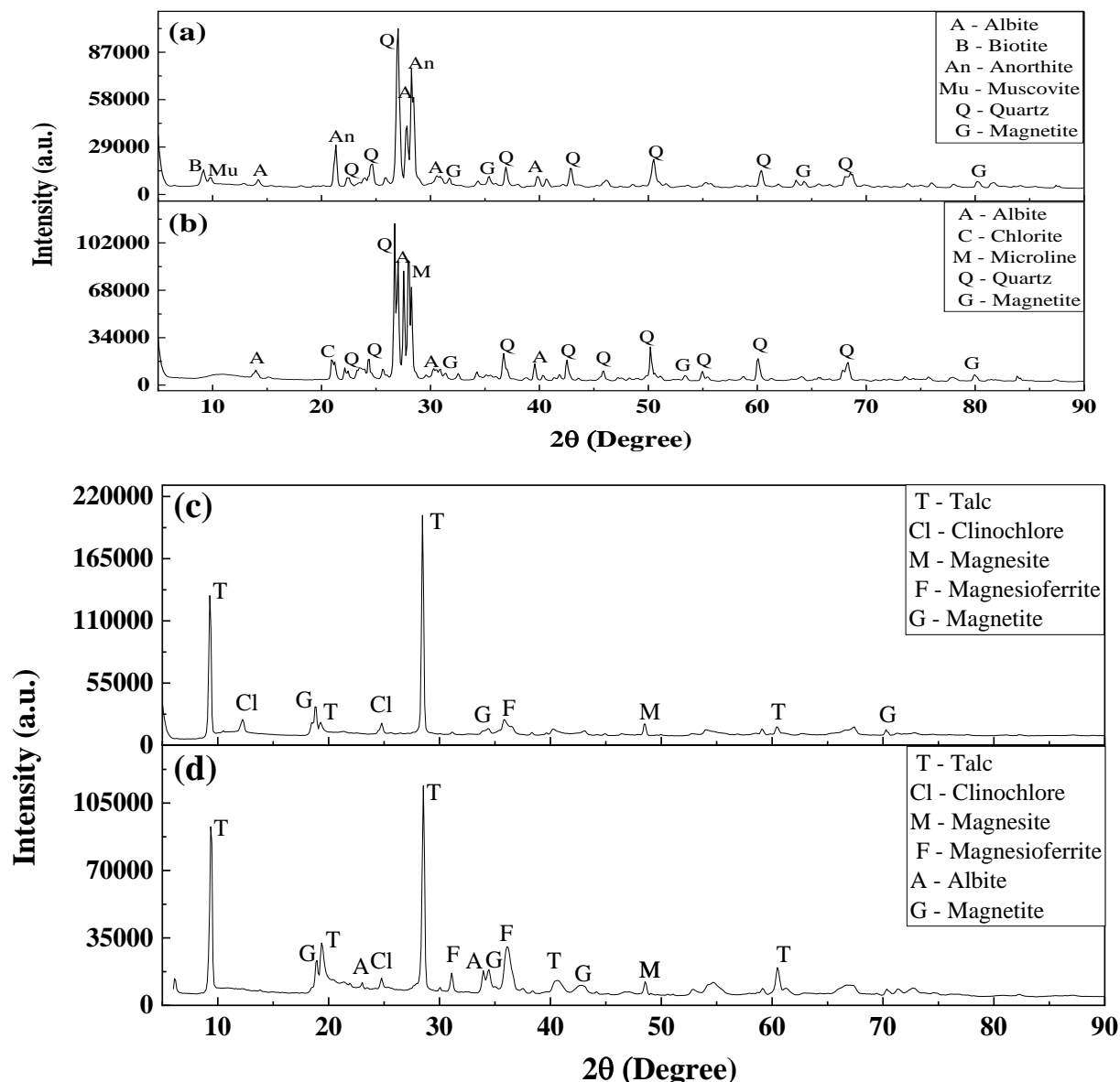


Figure 4: The XRD graphs for (a)CG, (b)UG, (c)CS and (d)US

The XRD images of soapstone rocks in Fig. 4(c) and (d) shows both rocks CS and US has peaks of Talc, magnesite ($MgCO_3$ with iron impurities), Magnesioferrite ($Mg(Fe^{3+})_2O_4$), Magnetite and Clinocllore ($(Mg,Fe^{2+})_5Al(Si_3Al)O_{10}(OH)_8$). The US rock also has albite in its composition. These results correspond to the oxide compositions in Figure 4 showing the relative sources of the variability in the percentages of iron oxides in the samples. The magnesite has a potential conversion to Mg-Fe oxide and recrystallisation which has a positive impact on the mechanical properties of the rock (Huhta *et al.*, 2019). Moreover, magnesite minerals have a high density of around 5.175 g/cm^3 which contributes to high densities and thermal capacity in soapstone rocks

(El Alami *et al.*, 2020). Huhta *et al.* (2016) also commends on the higher concentrations of magnesite and iron as a cause of elevated thermal shock resistance in soapstone rocks. These results show that CG rock will have poor chemical stability at elevated temperatures due to the presence of hydrothermal minerals. However, both soapstone rocks show a potential of having higher densities due to the presence of magnesite minerals.

4.2.3 Structural Analysis

Structural analysis enables the identification of the rock types and the determination of the structure of the rocks including the rocks mineralogy, grain size and foliation of the rock specimens (Nahhas *et al.*, 2019). The mineralogical compositions of the rocks are shown in Fig. 5. The rock CG is a coarse to medium igneous rock composed of quartz, albite, biotite and muscovite corresponding to a granite rock. Thomas *et al.* (2013) explains that the magmatic rocks in the Dodoma craton is characteristically grey and coarse grained. The mineralogical composition corresponds to the findings in Fig. 3, 4 and 6. The rock has black opaque areas corresponding to magnetite mineral ore. The UG is a fine to medium-grained igneous rock. It is composed of albite, microcline, opaque minerals, chlorite and quartz grains of variables sizes and shapes showing some alignment indicating that the rock is undergoing metamorphosis corresponding to the Meta-granite rock. Meta-granites are said to be common in the Ubendian and Usagaran belts as and impact of rock migmatization (Priem *et al.*, 1979; Ring *et al.*, 1997). The coarse to medium grained igneous rocks can be classified as intrusive rocks and are formed by a slower cooling of magma as compared to the medium to fine grained igneous rocks (Nahhas *et al.*, 2019). The increase in coarseness of the grains increase the porosity of the rocks and thus negatively affecting the density, thermal conductivity and overall strength of the rocks (Jones, 2003; Maqsood *et al.*, 2004).

The CS is a fine-grained, grey to green, soft with soapy texture, Soapstone. Dominantly composed of talc, with small amount of chlorite, magnesite, Magnesioferrite and opaque (magnetite) minerals. Rock US is a fine-grained, grey to green, soft with soapy texture. It has ultra-mylonitic foliation forming a porphyroblastic mix of inequigranular matrix of talc, magnesite and clinocllore surrounding the recrystallised albite. The ultra-mylonitic deformation is usually caused by plastic deformation that may possibly be due to the rocks being located in the Kiborian shear belt of the Usagaran which created deformation events that affected the metamorphic conditions (Fritz *et al.*, 2005). The foliation has a significant impact in reducing the thermal shock resistance of a rock (Huhta *et al.*, 2016) and lead fracturing after several thermal cycles (Allen *et al.*, 2014). Therefore, these results show that CS rock has a potential of high thermal shock resistance unlike the US rock. Additionally, the UG rock may have higher stability at higher temperature due to its migmatization.

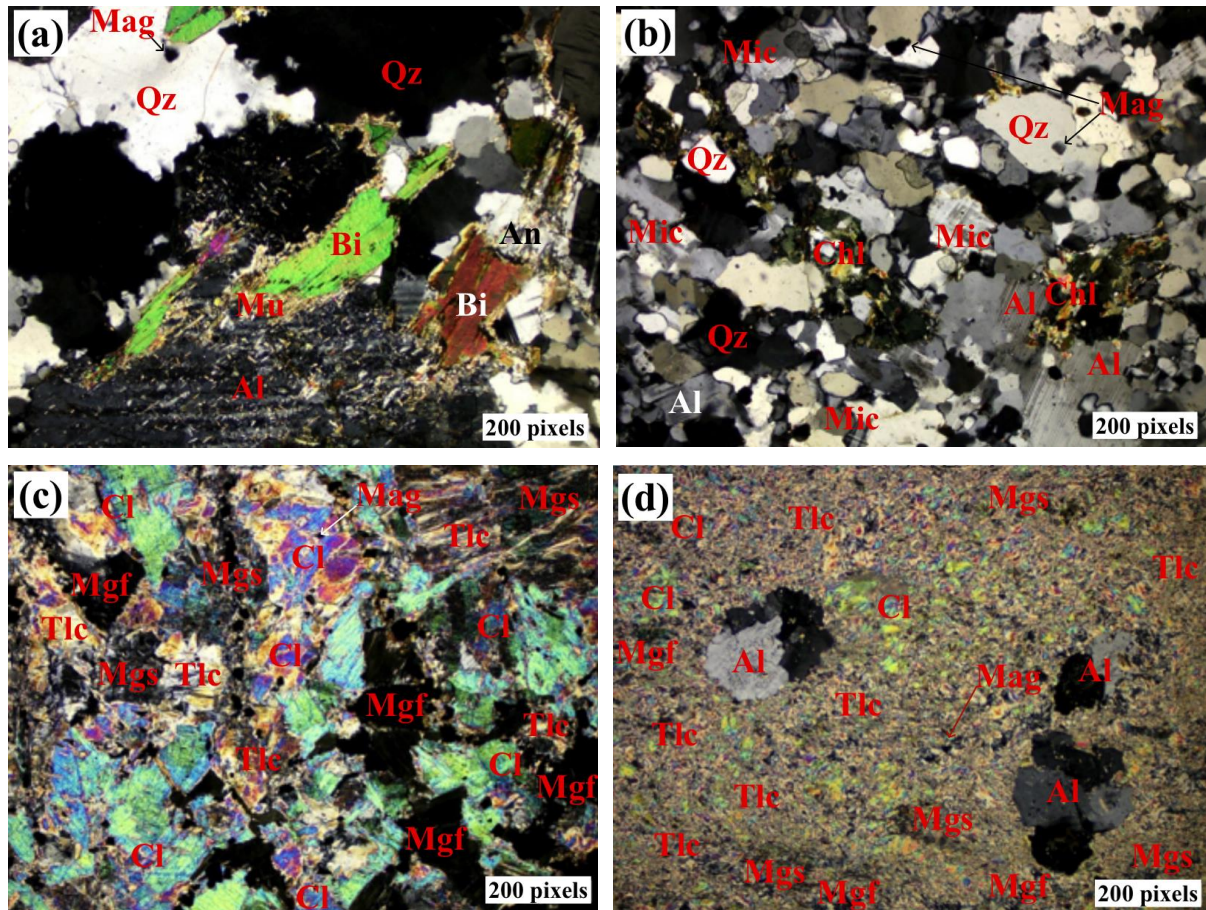


Figure 5: Petrographic image for (a)CG, (b)UG, (c)CS and (d)US.

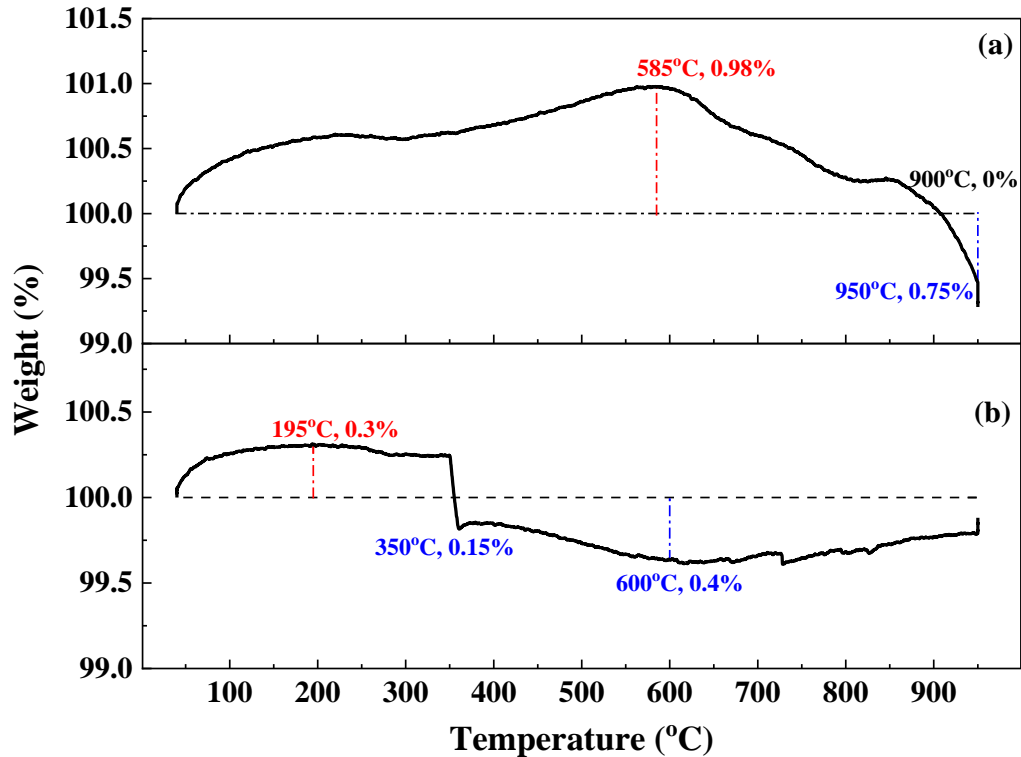
Whereby; Qz=Quartz, Mu=Muscovite, Bi=Biotite, Al=Albite, Chl=Chlorite, An=Anorthite, Tlc=Talc, Mgs=Magnetite, Cl=Clinchlore, Mag=Magnetite, Mgf=Magnesioferrite.

4.2.4 Thermal Gravimetric Analysis

The thermo-gravimetric analysis was performed for deducing the thermal stability and the volatility of the rocks' constituting materials with temperature increase (Alzahrani *et al.*, 2022). The weight changes with temperature for the rock samples are shown in the TGA graphs in Fig. 6. The TGA for the soapstone rocks CS and US are shown in Figure 8, and they show that the soapstone rock CS shows an increase in weight until it starts to have a lower weight below its initial percentage weight at 900°C to 950°C (which is above the solar drying and CSP temperature ranges) it undergoes a maximum weight loss of 0.75%. This weight loss is due to the release of the OH-molecules from the talc mineral that dominantly constitutes the rock (Pirinen, 2005). The high stability of CS rock may be due to its high-grade nature (formed in high temperature and pressure conditions) and the poly metamorphism of metamorphic rocks found in the Dodoma supergroup (Gabert, 1990). The soapstone US is stable at solar drying temperatures but loses weight until at total of 0.4% from the original weight at the high temperatures of 350°C to 600°C with no further weight loss thereafter. This weight loss is because US is a carbonate soapstone caused by the marine carbonate sediments of the oxic environment of the Usagaran belt as

compared to the CS that is of mafic origin (Godfray *et al.*, 2021; Moeller *et al.*, 1995). The carbonate undergoes chemical disintegration at higher temperatures of $300\text{ }^{\circ}\text{C} \leq t \leq 500\text{ }^{\circ}\text{C}$ to form an oxide and CO_2 that is released from the sample (Srinivasan *et al.*, 2020; Yavuz *et al.*, 2010).

The TGA for the granite rocks CG and UG are shown in Fig. 9, for CG there is a steep weight decrease of 1.2% at 100-250 $^{\circ}\text{C}$, due to the presence of Muscovite and biotite, the hydrothermal compounds that dehydrate by losing the chemically bound water at its boiling point (Alzahrani *et al.*, 2022; El Alami *et al.*, 2020). At 900-950 $^{\circ}\text{C}$ a total of 2.6% of initial weight is lost. Granite rock UG shows no weight loss throughout the temperature increase hence stable at both solar drying and CSP temperatures. It however shows an increase in weight due to the oxidation of mineral ores that are present in the sample. The trend of weight gain in granite has also been reported in (Alzahrani *et al.*, 2022). The stability of the UG rock at high temperatures is also contributed by the Usagaran migmatization process during the Pan-African thermotectonic episode that has metamorphised the original granite rock into a meta-granite (Priem *et al.*, 1979; Ring *et al.*, 1997). The CS, US, CG and UG rocks show a maximum mass gain of 0.98%, 0.3%, 0.5% and 0.3%, respectively. This is due to the oxidation reaction of magnetite mineral ore as shown in Fig. 6 and 7. The magnetite reacts with oxygen from the synthetic air to form hematite both at lower temperatures and at higher temperatures (Zheng *et al.*, 2021).



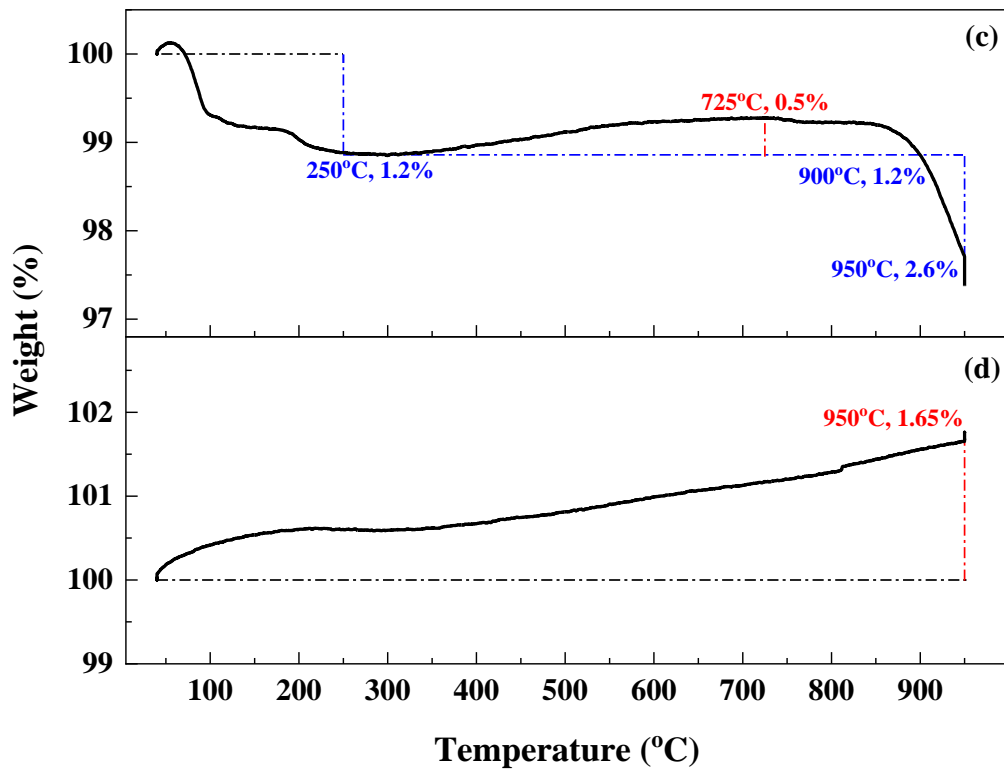


Figure 6: TGA graph for (a)CS, (b)US, (c)CG and (d)UG

The maximum service temperature (MST) of most TES materials are compared with those of the measured rocks as obtained in TGA experiment in Figure 7 as cited in Appendix 1. Of all the four experimented rocks UG had the highest MST of more exceeding 1000°C, other TES similar or exceeding 1000°C include HT concrete, high alumina concrete, brick magnesia, copper, aluminium, lead, cofalit and graphite. However, HT and high alumina concretes have inadequate thermal conductivities, brick magnesia has poor thermal shock while copper and aluminium have high investment cost and high thermal expansivity. Additionally, lead has inadequate thermal capacity despite is high investment cost, cofalit is expensive and difficult to produce and graphite reacts with carbon dioxide (CO₂) at higher temperatures and has low thermal capacity. Hence the TGA results indicate that the UG rock may have maximum service temperature above 1000°C since it did not show any weight loss and it exceeded more than 66% of other commonly used TES materials. The CS rock also show a good chemical stability up to 900 °C exceeding 62% of other commonly used TES materials. However, the US and CG rocks had weight loss at temperatures of 350°C and 250°C, respectively, exceeding only 8% of other commonly used TES materials.

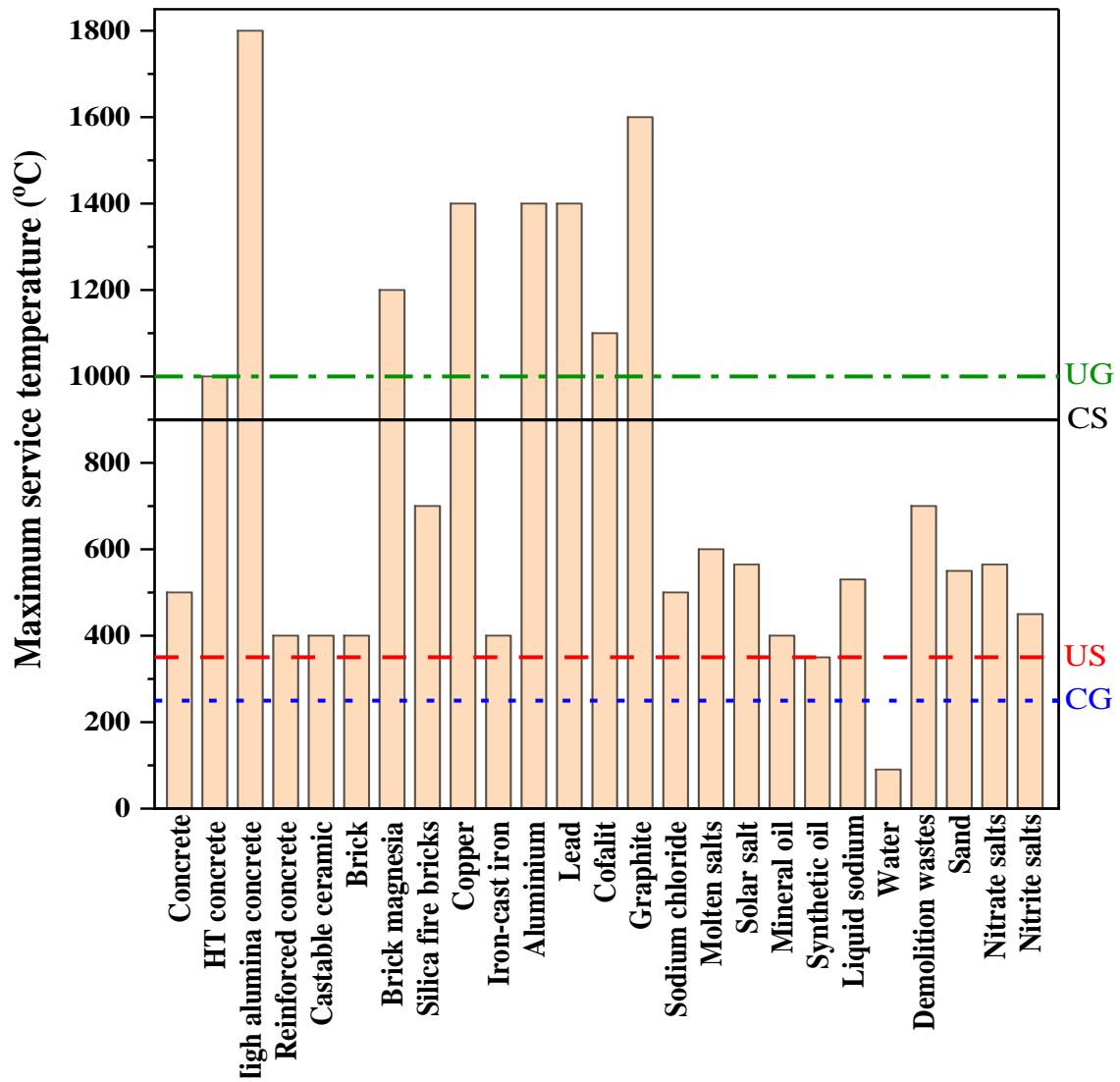


Figure 7: Comparison of maximum service temperature with other TES materials from literature

4.2.5 High temperature Test

High temperature test to understand the ability of the rocks to resist fracture caused by increase in temperature up to higher temperatures (Abdollahnejad *et al.*, 2020). The rock samples were heated up to temperature of 700°C and 1000°C as shown in Fig. 8. Soapstone samples had no visible cracks at both temperatures. However, granite rock CG had fractured and disintegrated at the temperature of 1000°C while rock UG had no visible cracks at that temperature. This may be attributed by the dehydration of the muscovite and biotite hydrothermal minerals which is a characteristic of granites rocks in the Craton geo-tectonic setting (El Alami *et al.*, 2020; Sun *et al.*, 2018) and the varying thermal expansion between quartz and other composing minerals are a contributing factor to the cracking of the CG rock (Hrifech *et al.*, 2019). Li *et al.* (2019) also observed that granite rocks develops cracks during the first thermo-cycle. Thus, all the rocks except CG prove to have a good thermal shock resistance.

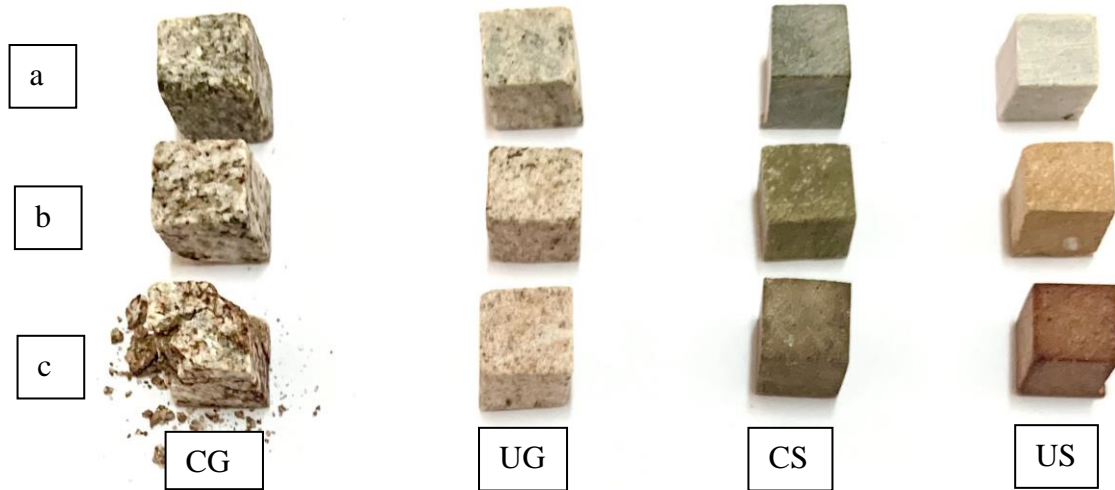


Figure 8: Rock samples: (a) ore, (b) heated at 700°C, (C) heated at 1000°C

4.3 Thermo-Physical Properties

4.3.1 Density and Porosity

Densities were determined so as to compare the expected containment volumes of the rocks in relation to amount of heat stored (Bal *et al.*, 2010) while porosity was measured so as to derive the amount of air spaces in the rock samples as they tend to affect conductance and mechanical properties of the rocks (Kant *et al.*, 2016; Rybacki *et al.*, 2015). Figure 9 shows that densities and porosities have an opposite relationship, where the density is lower with an increase in porosity. The densities and porosity are affected by mineral composition, chemical composition of minerals and the grain size (Huhta, 2019; Maqsood *et al.*, 2004). The densities of CG and UG were 2.228 g/cm³ and 2.426 g/cm³ while the porosities were 0.97 % Vol and 0.6 % Vol, respectively. This is because UG has fine grains hence a higher density and lower porosity as compared to CG rock. These porosity values of granite are in range those mentioned in literature i.e. 0.8-2.6 % Vol, while the density values are slightly lower than those mentioned in literature (Maqsood *et al.*, 2004; Tiskatine *et al.*, 2017).

Soapstone samples have higher densities as compared to granite samples, this was also observed in Huhta (2019) who explained that due to the ultra-mafic nature soapstone rocks tend to have elevated densities than other rocks, also this higher densities are brought about by the presence of magnesite compound that has a density of about 5.175 g/cm³ (El Alami *et al.*, 2020). Similarly, the densities and porosities are oppositely related. The CS rock has the highest density of 2.796 g/cm³ and the lowest porosity of 0.18 % Vol. High density and low porosity contributes to high thermal capacity of the rocks and higher thermal conductance of the rock (Kant *et al.*, 2016). The US rock has the highest porosity of 1.9 % Vol while its density is 2.635 g/cm³. High porosity has a negative effect on the compressive strength of rocks (Rybacki *et al.*, 2015). The porosity and

density values of soapstone correspond to the values reported in Hänchen *et al.* (2011) and Tiskatine *et al.* (2017) with the density of CS being slightly higher.

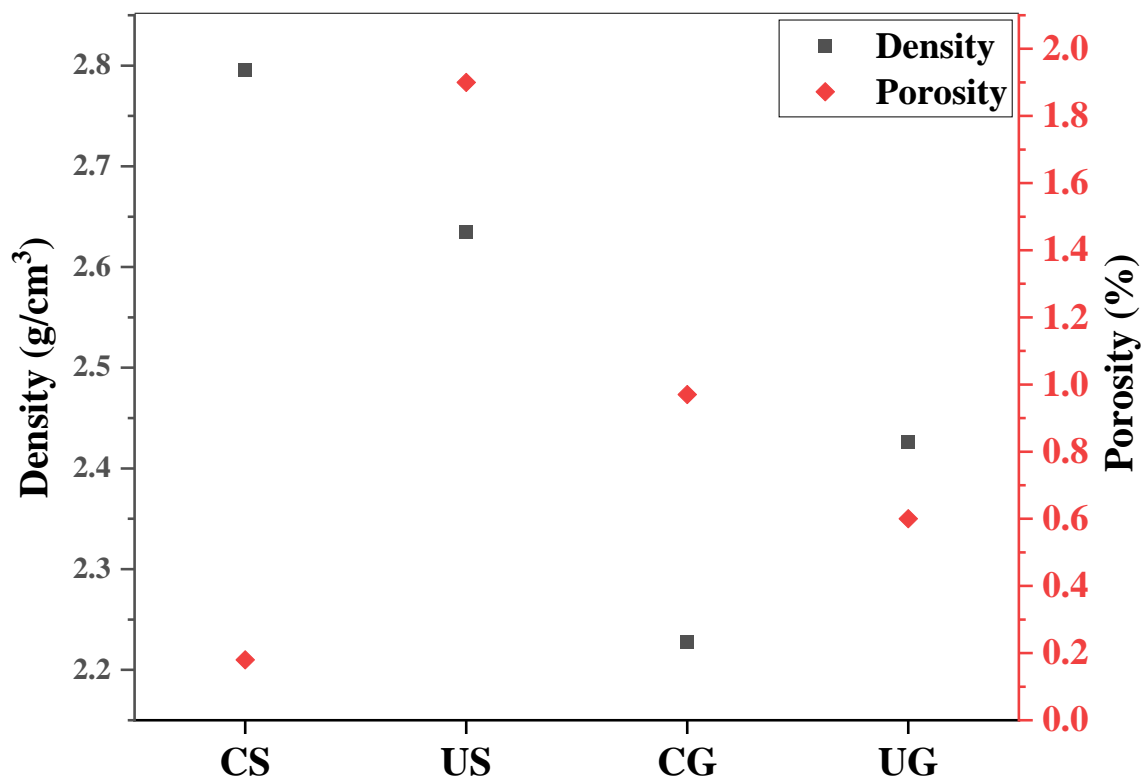


Figure 9: Density and porosity at room temperature

As compared to other rocks indicated in a study by Tiskatine *et al.* (2017) other rocks had higher porosities than the measured values with the highest being 8.06 % Vol for basalt rocks and 12.79 % Vol for schist rock while, quartzitic sandstone and rhyolite had the lowest porosity of 0.39 and 0.41 % Vol, respectively. The density values of other rocks are shown in Fig. 10 whereby, gabbro, basalt, dolomite and diorite rocks have the highest maximum densities of 3 g/cm³ and they exceed the density of CS significantly. The average density of dolerite and the maximum densities of marble and schist are almost similar to that of CS. Additionally, the densities of the rest of the rocks are in range with the values between CS, US, CG and UG. The minimum density of sandstone rock is 2.2 g/cm³ being the lowest value for all the rock types illustrated in Fig. 10.

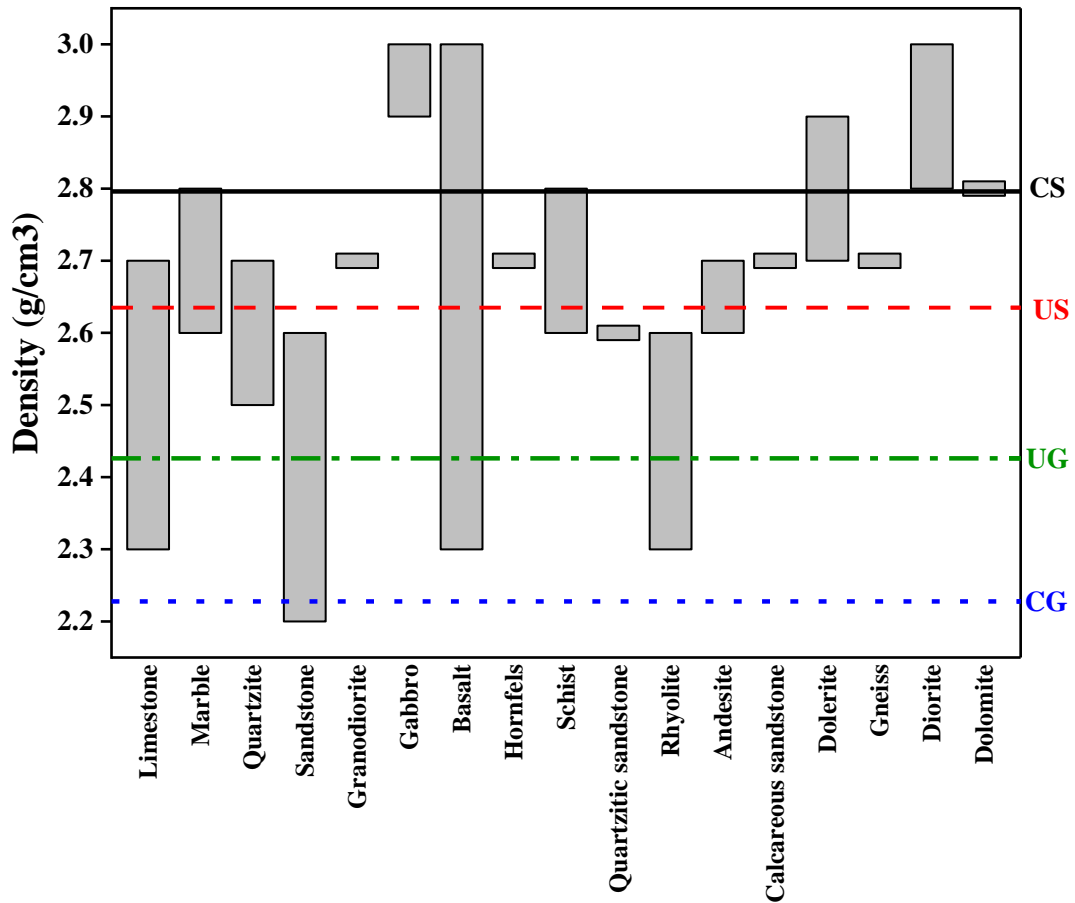


Figure 10: Comparison to the densities of other rocks from literature (Tiskatine *et al.*, 2017)

The densities of other common TES materials as obtained in literature referenced in Appendix 1 are shown in Fig. 11. Whereby, the metals copper, cast iron, and lead have very high densities ranging 7.9-11.3 g/cm³. However these metals require very high investment cost and lead has inadequate thermal capacity while copper and cast iron suffer from very high thermal expansion (Suresh & Saini, 2020). The densities of cofalit, brick magnesia, demolition wastes and all ceramics are 2.86-4 being slightly higher while, concrete, high tension concrete and aluminium have similar values with the CS rock. However, cofalit and the ceramics involve a very difficult and costly production process, brick magnesia suffers from poor thermal shock resistance and demolition wastes have poor thermal conductivities (Koçak *et al.*, 2020; Tiskatine *et al.*, 2017). Only the molten salts, graphite and high alumina concrete are in range with US, UG and CG rocks while, the remaining 12 materials have lower densities than the experimented rock samples with values between 0.8-2.2 g/cm³.

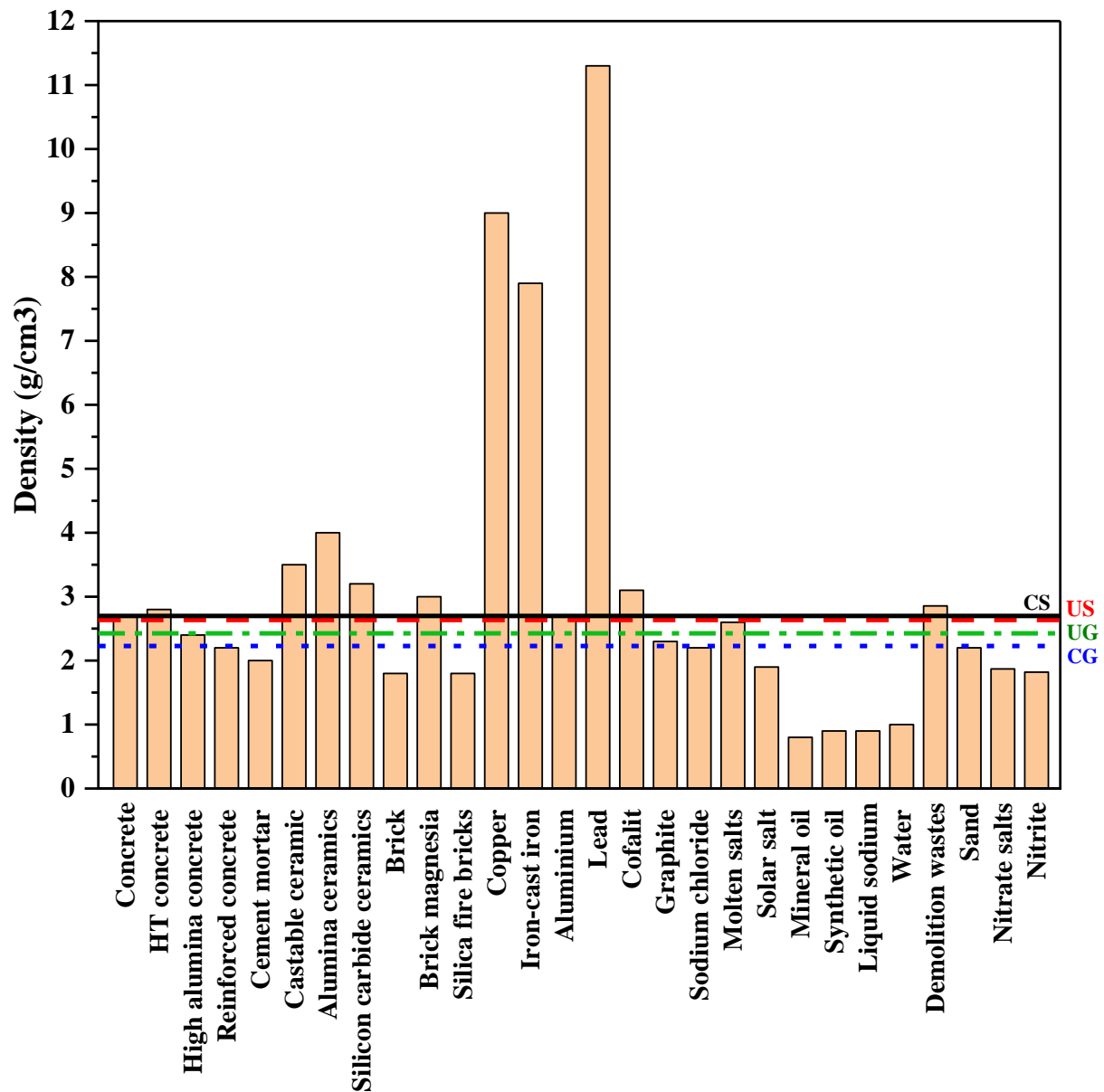


Figure 11: Comparison of density with other TES materials at room temperature

The evolution of density at low and high temperatures is as shown in Fig. 12 and 13. The density increase as the temperature increases is very insignificant concurring with findings reported by (El Alami *et al.*, 2020). In this study the density decreases with temperature increase at a very low rate of $7.53 \times 10^{-4} \text{ g}/(\text{cm}^3 \cdot \text{K})$ for rock CS, US and UG and $5.91 \times 10^{-4} \text{ g}/(\text{cm}^3 \cdot \text{K})$ for CG rock. Figure 12 shows that, at solar drying temperatures of 40 - 75°C the measured densities were 2.785 g/cm³, 2.635 g/cm³, 2.225 g/cm³ and 2.420 g/cm³ for CS, US, CG and UG, respectively, showing a slight decrease from the density at room temperature. The densities at CSP temperatures of 500 - 600°C for rocks CS, US, CG and UG were 2.77 g/cm³, 2.60 g/cm³, 2.2 g/cm³, 2.4 g/cm³ respectively as shown in Fig. 13. Zhu *et al.* (2022) observed the decrease of density with temperature as a courtesy of rock mass loss and volume increase due to expansion. In granite for example, the increase in volume is the leading factor due to high expansion rates of composing minerals especially quartz (Hrifech *et al.*, 2019; Zhu *et al.*, 2022). Therefore, the CS and CG rock shows a potential of having

the highest and lowest thermal capacities respectively courtesy of their density values. Lastly, the densities of rocks CS, US, UG and CG exceed thermal conductivities of other TES materials 57%, 54%, 50% and 36%, respectively.

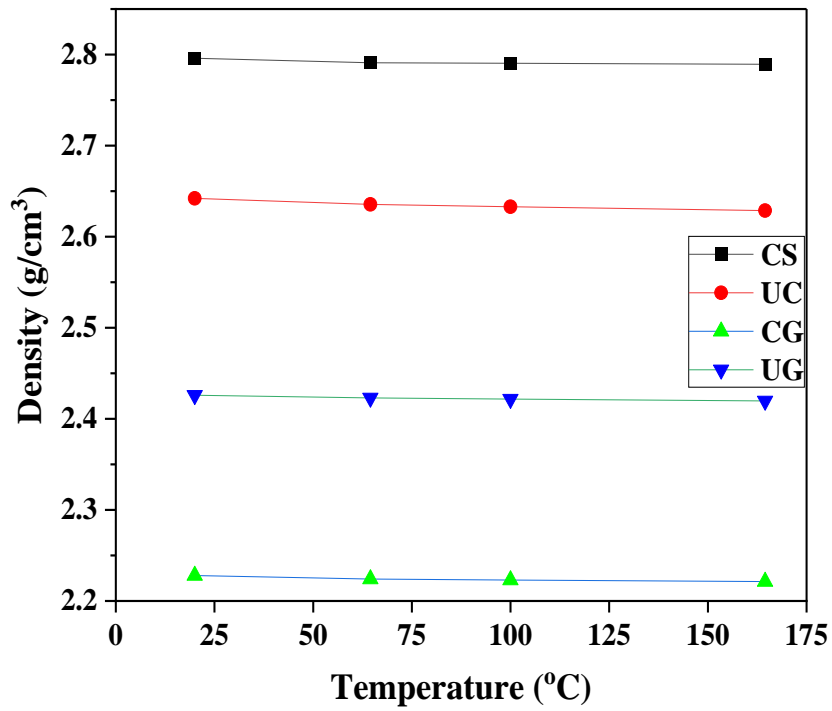


Figure 12: Evolution of density at low temperatures

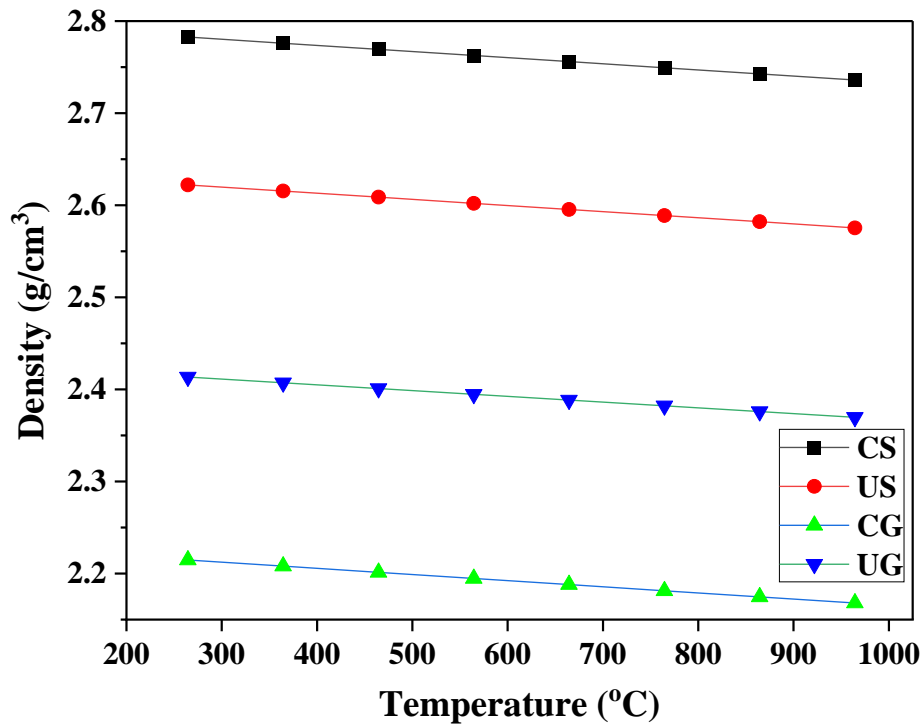


Figure 13: Evolution of density at high temperatures

4.3.2 Specific Heat Capacity and Thermal Capacity

(i) Specific Heat Capacity

The evolution of specific heat capacity from 20-950°C was measured so as to compare the expected amount of heat stored in a unit mass (Bal *et al.*, 2010). Specific heat capacities of the four samples are shown in Fig. 14 from which it can be observed that soapstone and granite rocks exhibit almost the same values. These similarities have also been reported by (Vosteen & Schellschmidt, 2003) where magmatic and metamorphic rocks exhibited almost same values of specific heat capacity with temperature changes. The magmatic granite rock samples CG and UG had the same values and trends to both metamorphic soapstone rock samples CS and US. Their evolution with temperature is as shown in Fig. 14, where the specific heat capacities increase with temperature. The increase in specific heat capacity at higher temperatures is slight, Nahhas *et al.* (2019) states that the slight increase is due to the Dulong-Petit law defining that the increase will eventually reach a constant value at higher temperatures. At 20°C the specific heat capacity of soapstone rock is 1.074 J/gK and of the granite rock is 1.07 J/gK. The increase in values between 200°C and 300°C is unexpectedly low, this was also observed by El Alami *et al.* (2020) and it was due to silanol transformation in which silicon hydroxide is converted to silicon oxide and aqua, the later then evaporates.

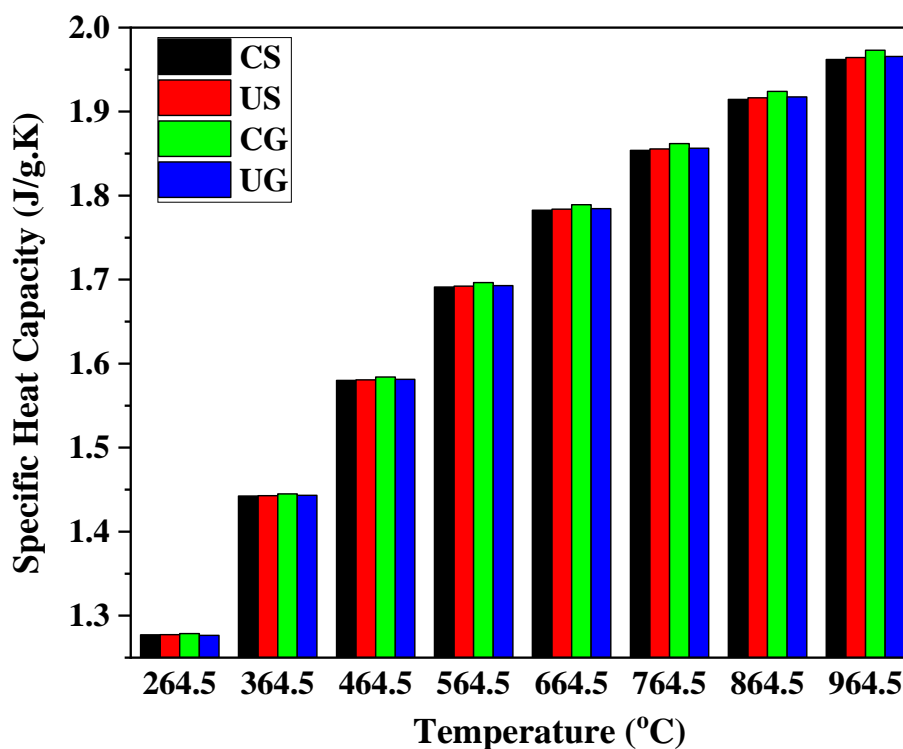


Figure 14: Evolution of specific heat capacity with temperature

As compared to most other rocks shown in Fig. 15, the specific heat capacity values of the experimented rocks at room temperature are higher. However, the maximum specific heat

capacities of basalt and schist are 1.23 J/gK and 1.1 J/gK which are higher than the experimented rocks. Diorite rock has the minimum specific heat capacity of 0.5 which is the lowest specific heat capacity value for all the rocks represented in Fig. 15.

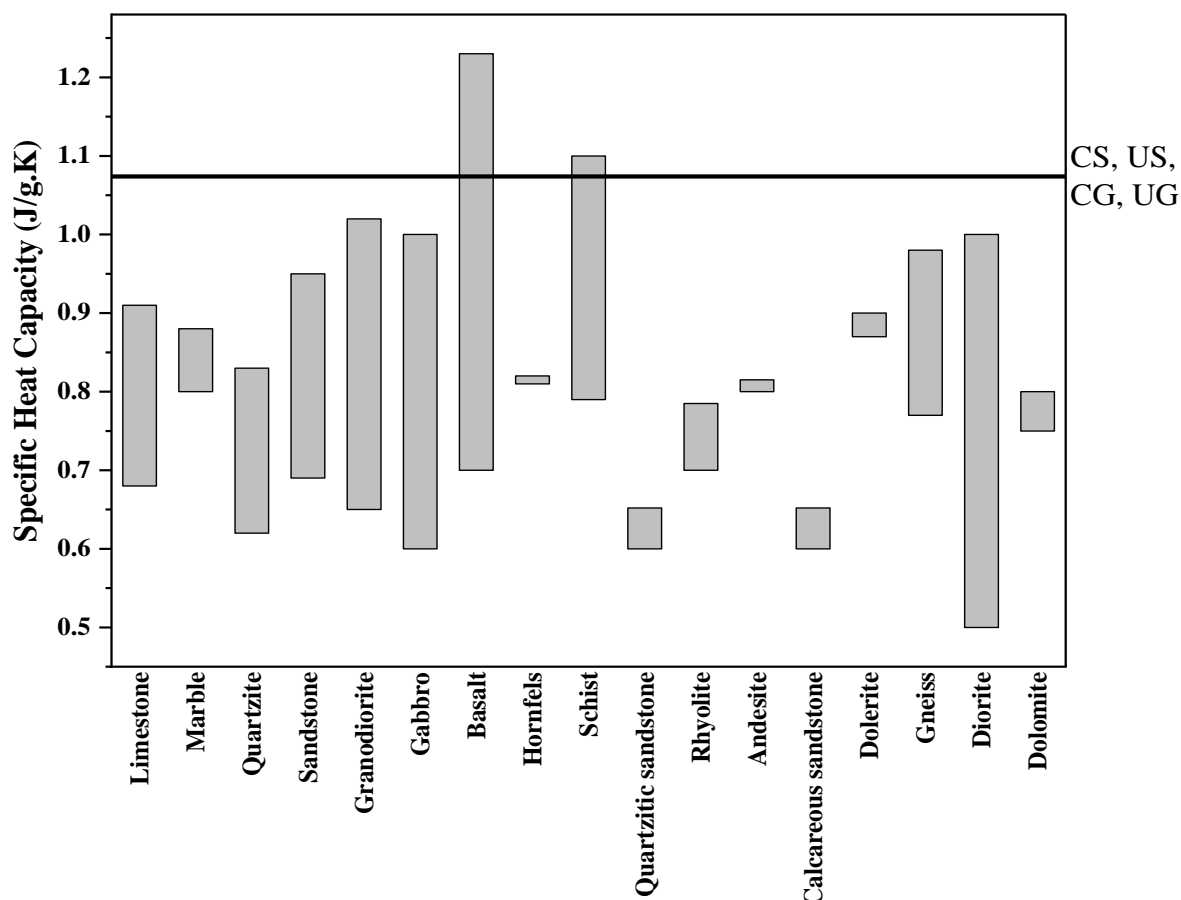


Figure 15: Comparison to the specific heat capacity of other rocks from literature (Tiskatine *et al.*, 2017)

The specific heat capacities of other common TES materials from the literature referenced in appendix 1 are shown in Fig.16, whereby water has the highest value amounting to 4.187 J/gK. However, Wang *et al.* (2020) reports that water suffers from very low thermal conductivity and a low maximum operating temperature of 90°C if used as stem it is highly corrosive to the plant and has an excessive vapor pressure. Other materials with higher specific heat capacities than the experimented rocks are mineral oil, synthetic oil, liquid sodium, demolition wastes, nitrate and nitrite salts with values between 1.13-2.6 J/gK. Nevertheless, mineral and synthetic oils have very low thermal conductivities, very high investment costs and short lifespan (Alva *et al.*, 2017; Zhang *et al.*, 2016). Lead has the lowest specific heat capacity of 0.131 J/gK. The specific heat capacity of all the experimented rocks is higher than those of 57% of other common TES materials.

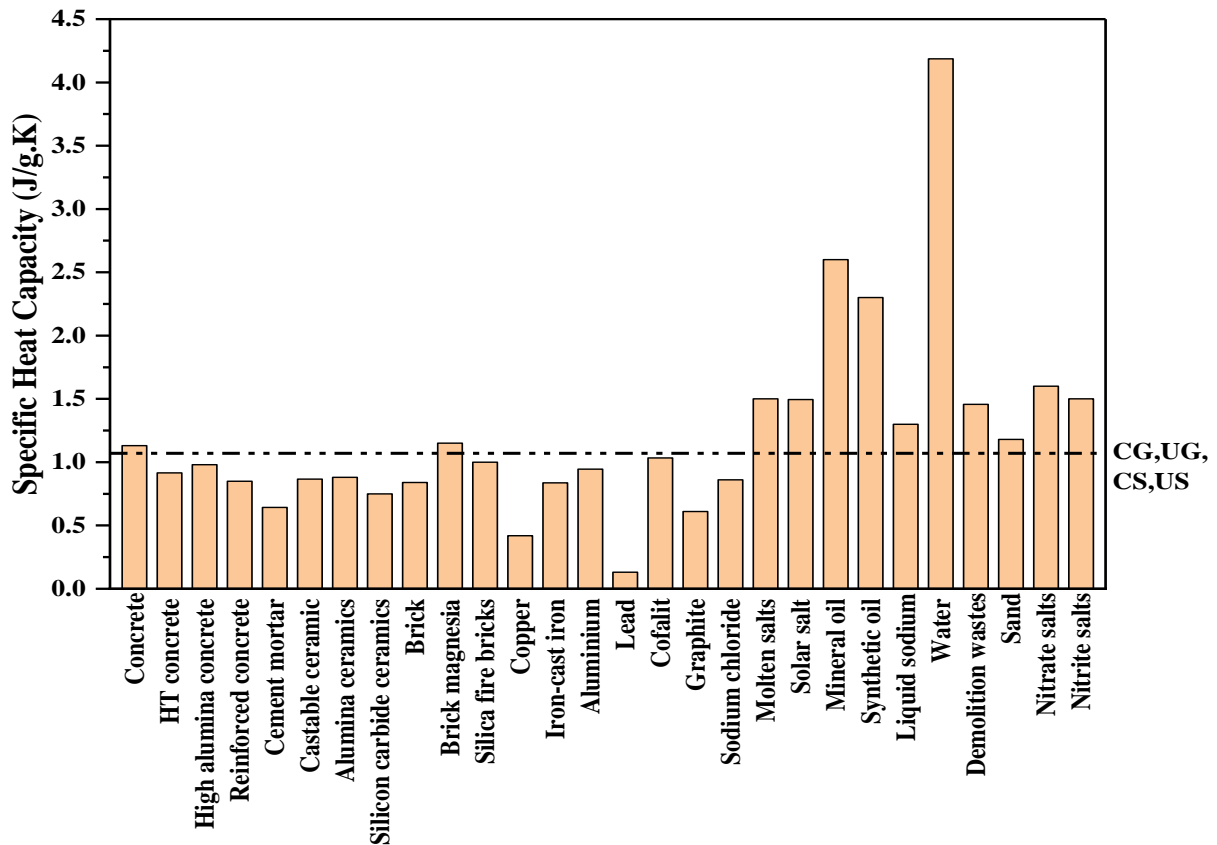


Figure 16: Comparison of specific heat capacity with other TES materials from literature

(ii) Thermal Capacity

The evolution of specific heat capacity from 20-950°C was measured so as to compare the energy densities of the rocks (Bal *et al.*, 2010). Thermal capacity at room temperature is as shown in Fig. 17 and 18, its evolution with temperature are as shown in Fig. 19 and 20. Since the thermal capacity is volumetric and the density changes very slightly with temperature the thermal capacity evolution follows almost the same profile as the specific heat capacity. However, the higher the density the higher the thermal capacity, hence the soapstone rocks and exhibited higher values as compared to the granite rocks. The thermal capacities of rocks CS, US, CG and UG were 3.0 MJ/(m³.K), 2.83 MJ/(m³.K), 2.4 MJ/(m³.K) and 2.6 MJ/(m³.K), respectively at 20°C.

Figure 17 also shows that quartzitic and calcareous sandstone, rhyolite, andesite and hornfels rocks have lower values than CS, US, CG and UG rocks. Most other rocks are having almost similar values to the range of experimented values. Gabbro, basalt and schist are potentially having maximum values that are slightly higher than CS. Basalt has the highest maximum thermal capacity of 3.75 MJ/(m³.K) and surprisingly the lowest minimum thermal capacity of all rocks of up to 1.5 MJ/(m³.K).

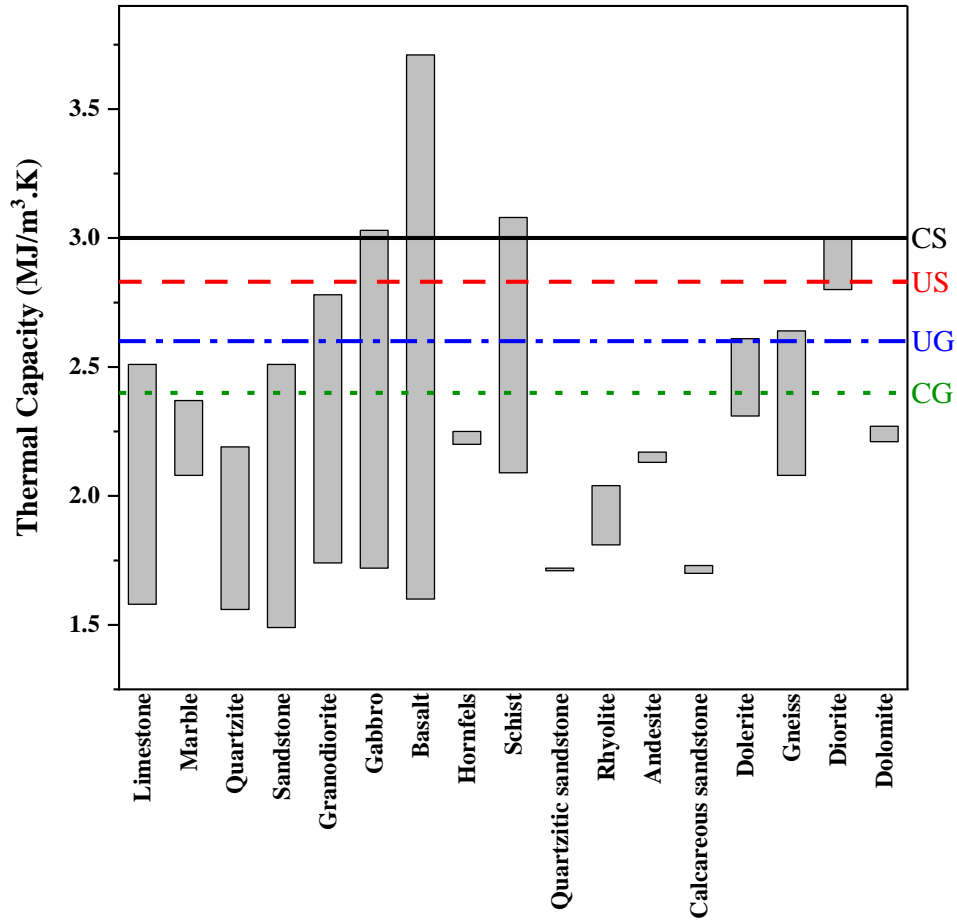


Figure 17: Comparison to the specific heat capacity of other rocks from literature (Tiskatine *et al.*, 2017)

Thermal capacities of other common TES materials are shown in Figure 18 as cited in Appendix 1. Whereby, alumina ceramics, Brick magnesia, copper, cast iron, cofalit, molten salts, water and demolition wastes have higher thermal capacities than the experimented rocks. Their thermal capacities range from 3.226-6.612 MJ/(m³.K). However, if used as TES materials alumina ceramics and cofalit are costly and are difficult to process, brick magnesia has poor thermal shock, copper and cast iron need high cost in investment and have a very high thermal expansion (Suresh & Saini, 2020; Tiskatine *et al.*, 2017; Zhang *et al.*, 2016).

Moreover, as previously discussed water suffers from very low thermal conductivity and a low maximum operating temperature of 90°C if used as stem it is highly corrosive to the plant and has an excessive vapor pressure (Wang *et al.*, 2020), while demolition wastes have inadequate thermal conductivity (Koçak *et al.*, 2020). Concrete, castable ceramics and nitrate salts have approximately similar thermal capacities to the CS rock. Nevertheless, castable ceramics and nitrate salts have poor thermal conductivity while nitrate salts high cost of investment (Wang *et al.*, 2020; Zhang *et al.*, 2016). The HT concrete, silicon carbide, aluminium, solar salt, sand and nitrite salt have thermal capacities ranging with the values between values of the four experimented rocks.

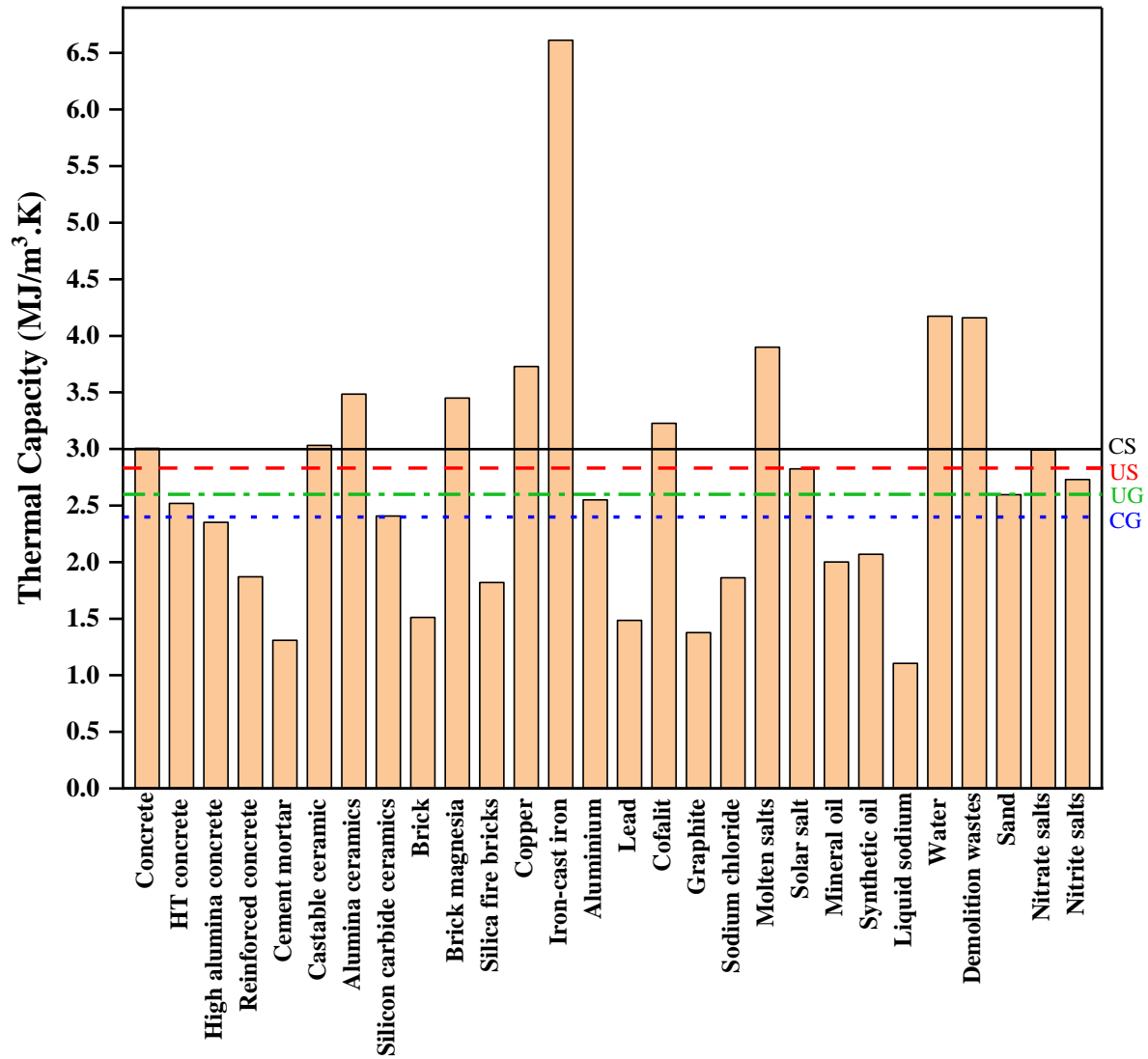


Figure 18: Comparison of thermal capacity with other TES materials from literature

At solar drying temperatures the thermal capacities ranged at 3.12-3.28 MJ/(m³.K), 2.94–3.1 MJ/(m³.K), 2.48-2.62 MJ/(m³.K) and 2.7-2.84 MJ/(m³.K) for CS, US, CG and UG, respectively as shown in Fig. 19. As the thermal capacities increase with temperature the values for concentrated power generation application are also higher as shown in Figure 20. These values ranged at 4.45-4.65 MJ/(m³.K), 4.25-4.45 MJ/(m³.K), 3.55-3.8 MJ/(m³.K), 3.9-4.15 MJ/(m³.K) for CS, US, CG and UG, respectively. This trend of thermal capacities increase with increase in temperature was also observed in Bouvry et al. (2017) and Nahhas et al. (2019). The results thus show that the thermal capacity for CS rock is the highest both at room temperatures and at elevated temperatures.

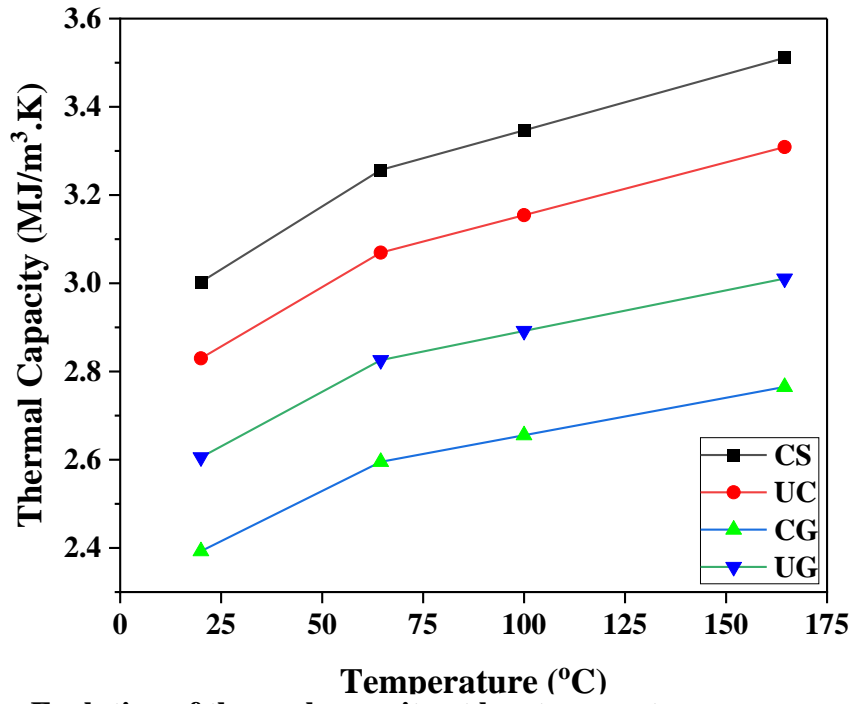


Figure 19: Evolution of thermal capacity at low temperatures

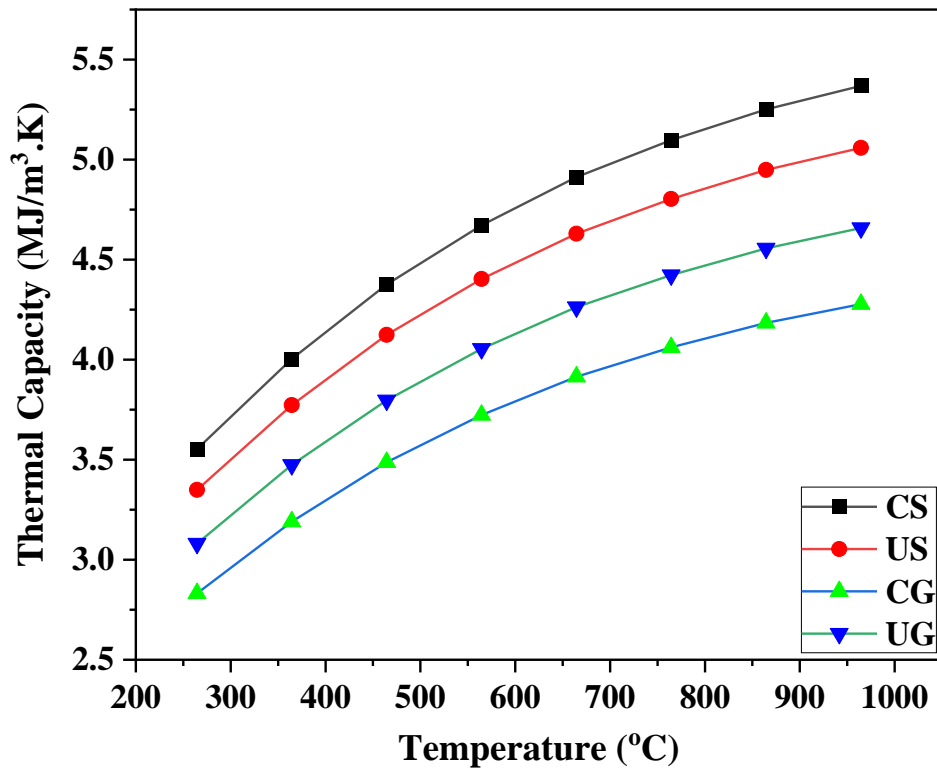


Figure 20: Evolution of thermal capacity at higher temperatures

4.3.3 Thermal diffusivity and Conductivity

Thermal diffusivity and thermal conductivity were determined so as to understand the rates of thermal charging and discharging of the rock samples (Bal *et al.*, 2010).

(i) Thermal Diffusivity

Thermal diffusivity of the samples decreases with temperature as shown in Fig. 21 and 22. This observation has also been reported by (El Alami et al., 2020). The diffusivity values of soapstone are higher than those of granite at room temperature and at elevated temperatures. Lower values of diffusivity implies that the rock has a tendency to absorb heat as opposed to transmitting it for the required use (Nahhas *et al.*, 2019). At 20°C soapstone diffusivity values for CS and US samples are 0.86 mm²/s and 0.77 mm²/s, respectively while the values for granite samples CG and UG at the same temperatures are 0.70 mm²/s and 0.73 mm²/s. At 300°C the diffusivity of CS, US, CG and UG falls at a difference of 0.2 mm²/s, 0.18 mm²/s, 0.14 mm²/s and 0.18 mm²/s, respectively. Making the average rate of change of diffusivity to be 0.001 mm²/s°C for soapstone and 0.0008 mm²/s°C for granite. This is because the rate of decrease is higher to rocks with higher values at room temperature as opposed to those with lower values (El Alami *et al.*, 2020).

Figure 21 shows that at 40-75°C where solar drying is convenient, the diffusivity of the rocks decreases up to a range of 0.825-0.775 mm²/s, 0.745-0.71 mm²/s, 0.675-0.645 mm²/s and 0.705-0.67 mm²/s for of CS, US, CG and UG respectively. Figure 22 displays that although the rate of decrease in diffusivity of soapstone is higher than of granite, the overall diffusivity values for granite at 300°C are relatively lower than those of soapstone. At CSP temperatures ranging 500-600°C, the diffusivity of the rocks ranges at 0.54-0.505 mm²/s, 0.48-0.425 mm²/s, 0.45-0.4.5 mm²/s and 0.455-0.42 mm²/s for of CS, US, CG and UG respectively. At 700°C and above the diffusivity of soapstone CS is highest while the diffusivity of soapstone US is almost similar to that of granite UG and CG. The high diffusivity at higher temperatures in CS may be attributed by the presence of hematite in soapstone CS (Nahhas *et al.*, 2019). Since thermal diffusivity and thermal conductivity are directly proportional (Bouvry *et al.*, 2017), CS rock shows a potential of having the highest thermal conductivity while CG may have the lowest.

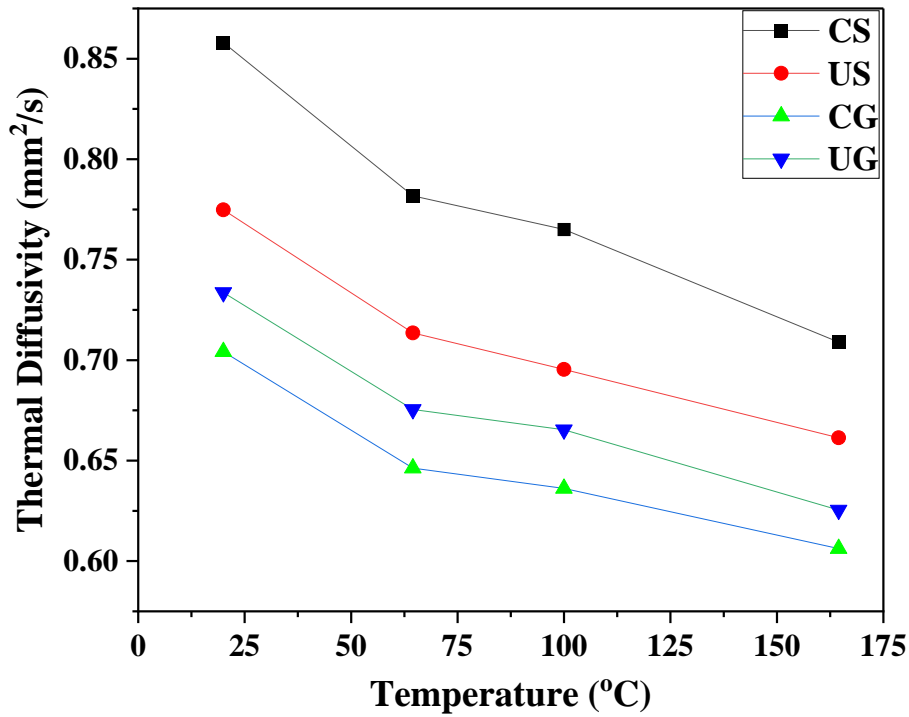


Figure 21: Thermal diffusivity at low temperatures

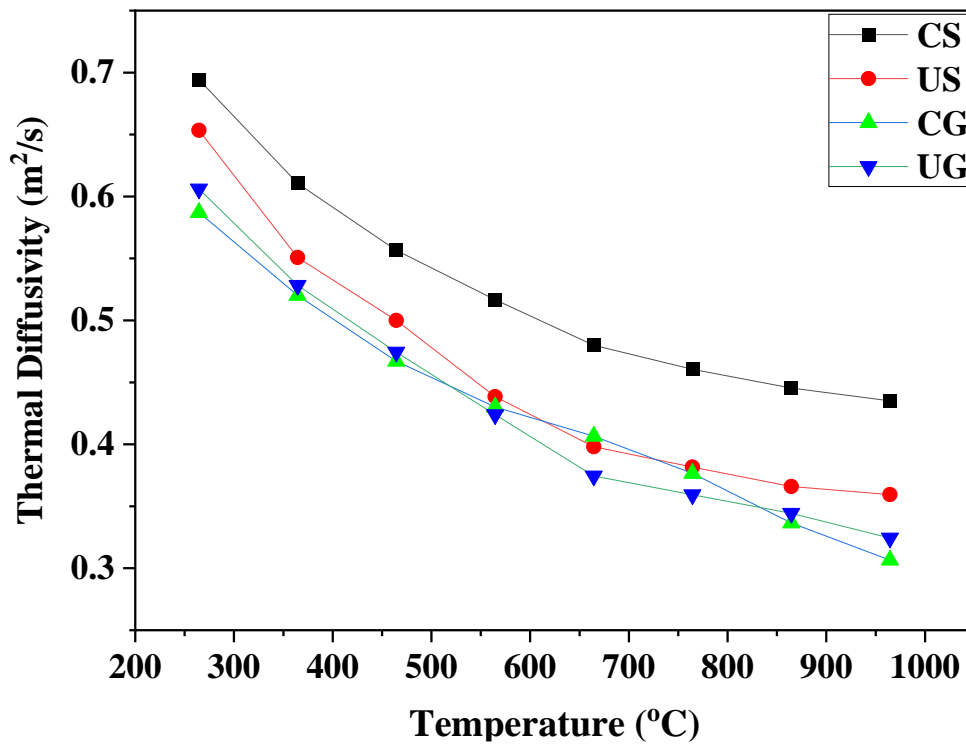


Figure 22: Thermal diffusivity at high temperatures

(ii) Thermal Conductivity

Thermal conductivity for the four samples at room temperature is as shown in Fig. 23 and 24. Thermal conductivities at 20°C were 2.58 W/(mK) and 2.19 W/(mK) for soapstone CS and US respectively while those of granite CG and UG were 1.69 W/(mK) and 1.91 W/(mK). The conductivities for soapstone were higher than those of granite. The thermal conductivities of

soapstone are in range to those stated in Tiskatine *et al.* (2017) on the contrary to granite whose both values are lower and this may be contributed by the low density of the rock samples.

Thermal conductivities of most other rocks are shown in Fig. 23. Quartzite rock quartzitic and calcareous sandstones rocks that have higher values ranging between 2.85-5.75 W/(mK). Limestone, marble, sandstone, hornfels, schist, Andesite, dolerite and gneiss have their values ranging within the experimental measured values but with their maximum values exceeding the measured values of the four measured rocks, spanning from 1.7 W/(mK) to 3.2 W/(mK). The lowest thermal conductivity in rocks is that of basalt with the minimum value of 1.2 W/(mK).

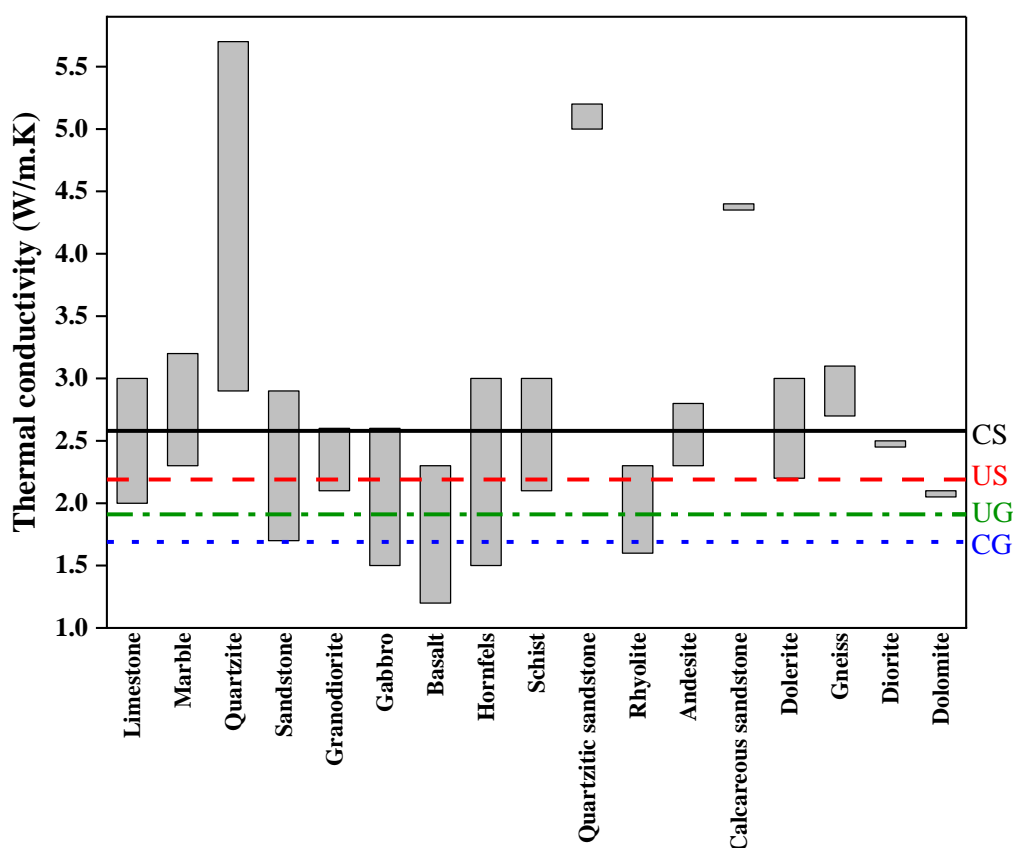


Figure 23: Comparison to the thermal conductivities of other rocks from literature (Tiskatine *et al.*, 2017)

Thermal conductivities of other common TES materials are shown in Fig. 24 as cited in Appendix 1. whereby, alumina ceramics, silicon carbide ceramics, brick magnesia, copper, cast iron, aluminium, lead, cofalit, graphite, sodium chloride and liquid sodium have higher thermal conductivity values than all the four experimented values ranging from 2.7-385 W/(mK). Furthermore, concrete, HT concrete, reinforced concrete, castable ceramics, silicon fire bricks, molten salts, solar salts, cement mortar, brick, water, demolition wastes, nitrates and nitrite salts have values less than CS but range within the values between the four measured values.

As displayed in Fig. 25, the thermal conductivity generally decreased with temperature. This is

caused by the crystalline nature of the rocks as shown in the peaks of the XRD in Fig. 4. Nahhas *et al.* (2019) explains that, for crystalline rocks the conductivity decreases with temperature as opposed to the amorphous rocks in which the diffusivity usually increases with temperature. at lower temperatures the rate of decrease of thermal conductivity is higher in CS rocks than in the other three rocks but at higher temperatures shown in Fig. 26, its rate of decrease is the lowest compared to US, CG and UG rocks. Chen *et al.* (2021) explained that the rate of decrease of thermal conductivities is dependent on the its values at room temperature where by conductivities between 2.5 and 3.5 W/(mK) will show a linear decrease while those below 2.5 W/(mK) will have a minor decrease at lower temperature and a significant decrease at higher temperatures. Thus, the Soapstone sample CS showed significantly higher conductivity values at higher temperatures as compared to US, CG and UG rocks. At 40-75°C (solar drying temperatures) the average conductivities of CS, US, CG and UG are 2.56 W/(mK), 2.19 W/(mK), 1.65 W/(mK) and 1.95 W/(mK), respectively (Fig. 25). While at CSP temperatures of 500-600°C the conductivity values for the rocks as shown in Fig. 26 were 2.42 W/(mK), 2 W/(mK), 1.6 W/(mK) and 1.72 W/(mK), respectively. Confirming that the rate of heat transfer in rocks is expected to be higher during solar drying applications than in CSP applications. Since the thermodynamic capacity in terms of charging and discharging increase with an increase in thermal conductivity (Tiskatine *et al.*, 2017), CS rock has a potential of having the best performance thermodynamically than other three experimented rocks while CG rock may have the lowest. The rocks CS, US, UG and CG exceed thermal conductivities of other TES materials 61%, 46%, 36% and 11%, respectively.

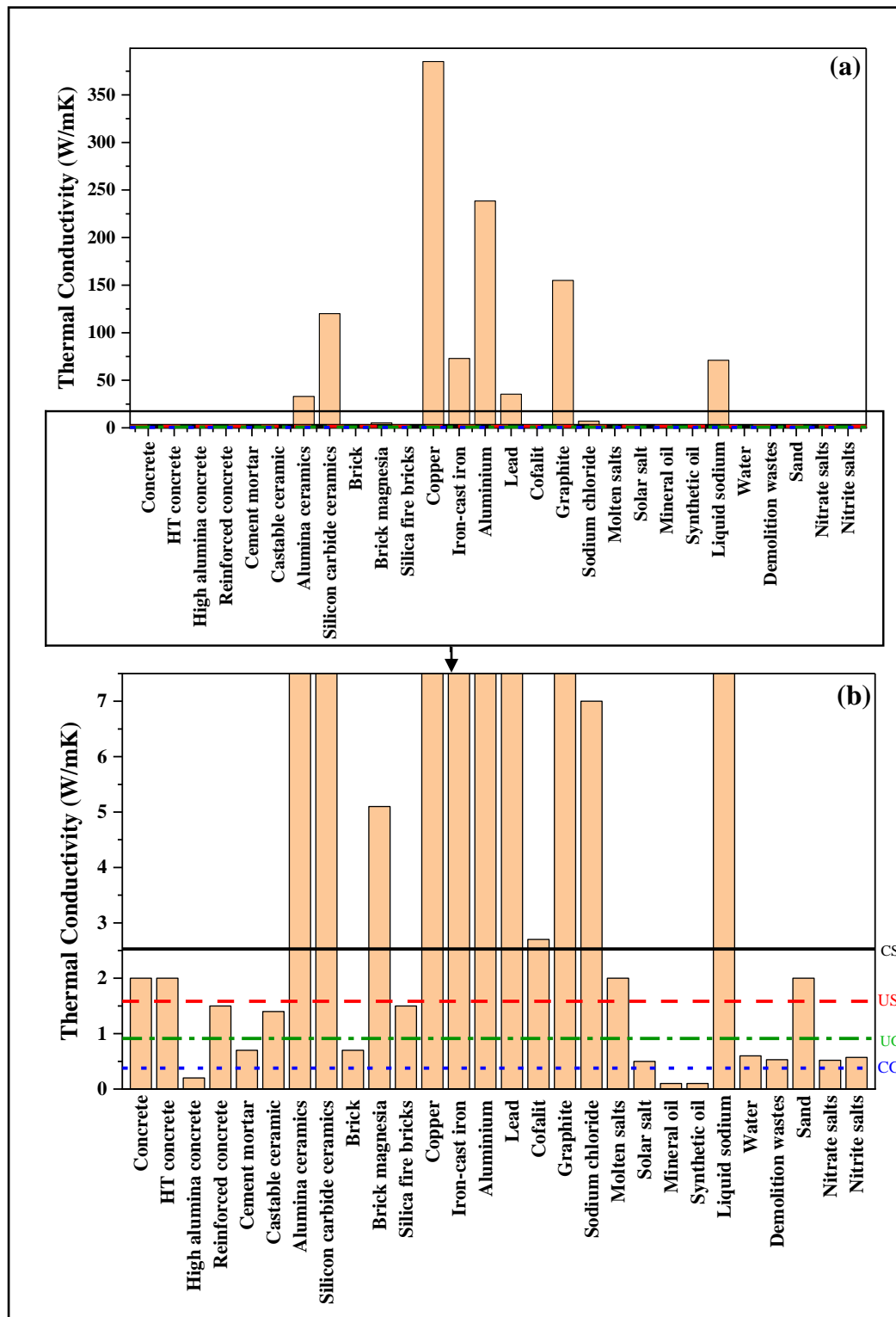


Figure 24: Comparison of thermal conductivity with other TES materials from literature
 (a) scale ranging 0-400 W/mk (b) scale zoomed to 0-7 W/mk

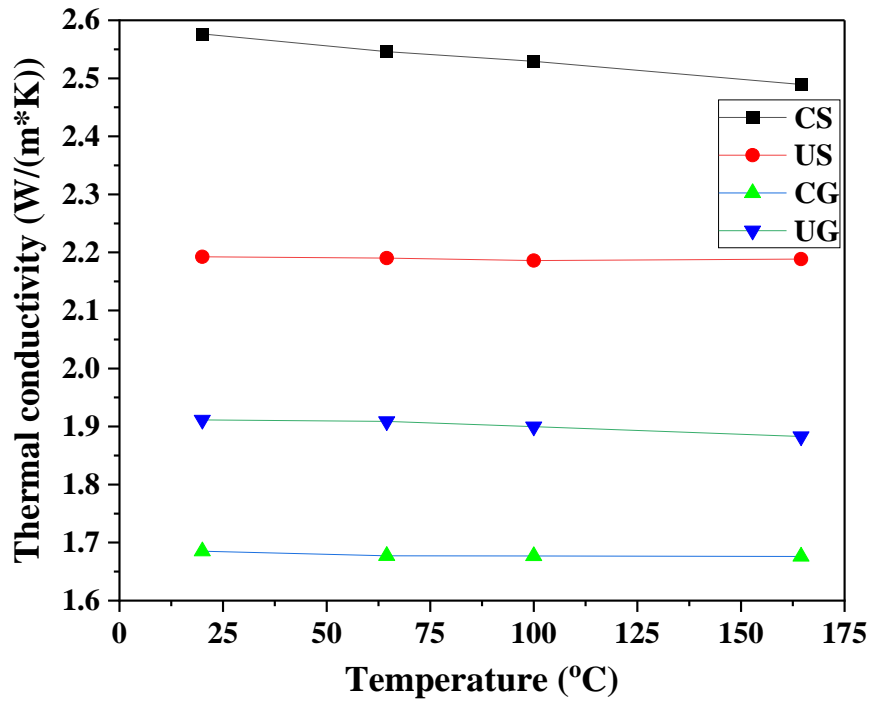


Figure 25: Thermal conductivity at low temperatures

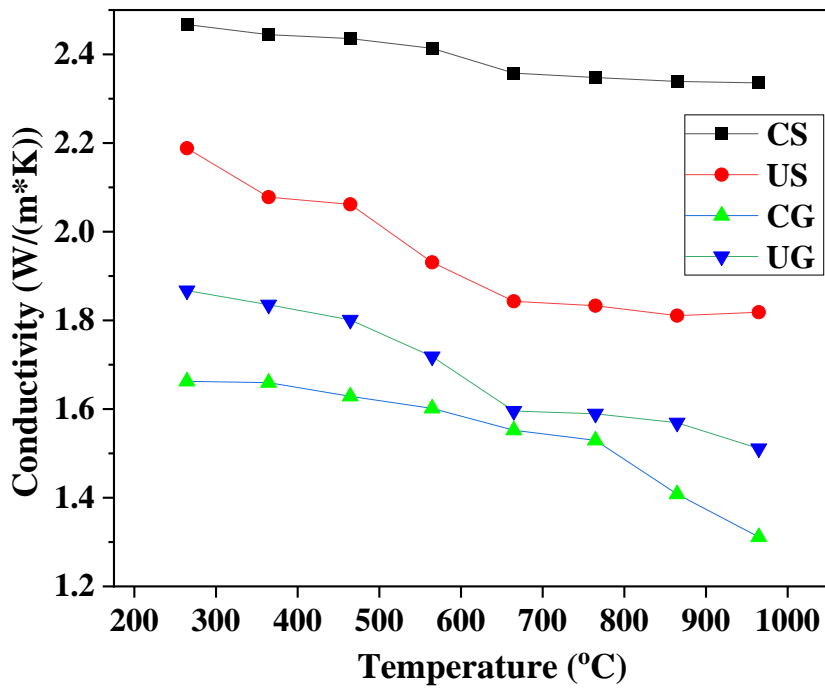


Figure 26: Thermal conductivity at high temperatures

4.4 Thermo-Mechanical Properties

4.4.1 Young's Modulus

The Young's modulus was determined so as to deduce the heterogenous ability of the lower layer of rocks to withstand the point loading from upper layer of rocks (Borodich *et al.*, 2015; Nahhas *et al.*, 2019). Figure 27 shows the Young's modulus of the four rock samples as a measure of their

mechanical strength on point loading since, point loads are usually higher than overall distributed loading in rock beds (Allen *et al.*, 2014). Despite its high heterogeneity, the soapstone rock CS had the highest value of 135 GPa followed by the granite rocks UG and CG that have Young's modulus mean values of 95 GPa and 104 GPa, respectively. The values of Young's modulus for CS, CG and UG are above 80 GPa a value that was recommended by Nahhas *et al.* (2019) for TES materials. However, the soapstone rock US has a low unrecommended value of 60 GPa, and this is due to its meta-sedimentary nature of its origin and its high porosity (Begg *et al.*, 2009; Rybacki *et al.*, 2015). Since the young modulus results are $US < 80 \text{ GPa} < CG < UG < CS$ then the US rock has insufficient compressive strength for TES applications and CS has the best compressive strength.

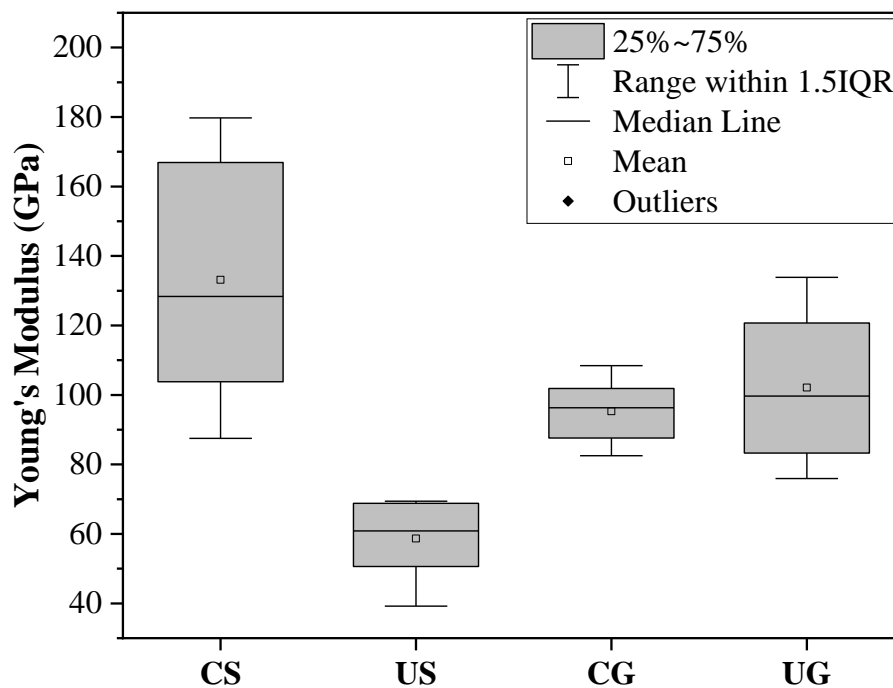


Figure 27: Young modulus at room temeperature

CHAPTER FIVE

CONCLUSION AND RECOMMENDATIONS

5.1 Conclusion

This work studies the variation in the thermal energy storage properties of two types of natural rocks, granite and soapstone, as collected from two different geo-tectonic settings of Craton and Usagaran. The use of rocks as materials for the storage of sensible heat in solar application at solar drying and CSP temperatures is a viable and cost-effective alternative to deal with the inherent variability of the solar resource for thermal applications. Experimental characterisation was performed to investigate the thermo-chemical properties (thermal stability (TGA), crystalline phases (XRD), petrographic imaging and chemical composition (XRF), and high temperature test); the thermo-physical properties (density, porosity, specific and thermal capacity (DSC), thermal diffusivity, and conductivities (LFA)); and the thermo-mechanical properties (Young's modulus) of the rocks.

The collected data shows a significant difference between the soapstone and granite rocks from Craton and Usagara geotectonic settings. The chemical compositions in granites had less variation as opposed to the mineral composition where CG contained hydrothermal minerals and UG had only thermally stable minerals. Soapstone had a variation in chemical compositions that confirmed that CS is an ultramafic rock and US a carbonate soapstone however, they had similar minerals that varied only in terms of intensities. The TGA results showed that maximum weight loss for CG, US and CS were 1.2% at 100-250°C, 0.4% at 250-350°C, 0.75% at 950-980°C, while UG had no weight loss throughout the temperature range of 40-950°C.

The premature chemical disintegration in CG and US was due to the loss of water in the hydrothermal minerals and the decomposition of carbonates into carbon dioxide, respectively. The Young's modulus for US, CG, UG and CS at room temperature were at 60, 95, 104, 135 GPa showing that US rock is mechanically incapable as a TES material. The energy densities (thermal capacities) and the rates of heat transfer (thermal conductivities) were consistently at $CS > US > UG > CG$. At solar drying temperatures, the thermal capacities and conductivities ranged at 2.7-3.28 MJ/(m³.K) and 1.91-2.56 W/(mK), respectively. At CSP temperatures they ranged at 3.9-4.65 MJ/(m³.K) and 1.68-2.43 W/(mK), respectively. The CG rock fractured and disintegrated during the high temperature fracture test at 1000°C while CS, UG and US showed no cracks due to their high thermal shock resistance.

The overall results show thermal properties for both soapstone and granite vary with geo-tectonic

settings and are site specific. The soapstone from craton (CS) have good performance as a thermal energy storage material for both CSP and solar drying surpassing the other three rocks in terms of thermal capacity and conductivities which contribute to good absorption hence good storage and transmission of heat per degree change in temperature. It also has a good chemical stability at higher temperatures and has the highest mechanical strength. The soapstone from Usagara had the second-best thermal capacity and thermal conductivities but are susceptible to deterioration at elevated temperatures and have the lowest mechanical strength and thus are easiest to disintegrate due to rock-bed loading. The UG rock has low thermal capacity and conductivity thus needing a high temperature change to store an equally amount of energy to the soapstone rocks. Despite its good mechanical and chemical properties, it is insufficient for solar drying since high temperatures above 75°C negatively impact the nutritional values of the dried foods. In addition to these drawbacks the CG rock undergoes chemical disintegration at solar drying temperatures.

5.2 Recommendations

There is a need to conduct further experimentation to examine the actual TES performance capacity of these rocks through charging and discharging experiments. Moreover, Tanzania has a variety of rocks situated in various geo-tectonic settings hence, the study of rock variability as TES materials with geotectonic settings for other types of rocks should also be done so as to study the patterns and trends of these variations.

There is a need to study the variability of rock properties as per geo-tectonic settings. Most literature on geo-tectonic settings in Tanzania are based on the ages of rock formation and type and composition of rocks present and none studied the physical and mechanical properties variabilities. Hence, missing crucial data on how these variable chemical and geological properties of the rocks may influence the physical and mechanical properties as per geo-tectonic setting of origin.

REFERENCES

- Abdollahnejad, Z., Mastali, M., Rahim, F., Luukkonen, T., Kinnunen, P., & Illikainen, M. (2020). 29 - Influence of cobinders on durability and mechanical properties of alkali-activated magnesium aluminosilicate binders from soapstone. In P. Samui, D. Kim, N. R. Iyer, & S. Chaudhary (Eds.), *New Materials in Civil Engineering* (pp. 877-895). Butterworth-Heinemann. <https://doi.org/https://doi.org/10.1016/B978-0-12-818961-0.00029-6>
- Adeleke, A., & Airoboman, A. (2019). A Review on Packed Bed of Rock as Thermal Energy Storage for Concentrated Solar Power Plant. *International Journal of Engineering Research*, 8, 121-130.
- Aladejare, A., & Wang, Y. (2016). Evaluation of rock property variability. *Georisk*, 11. <https://doi.org/10.1080/17499518.2016.1207784>
- Allen, K., von Backström, T., Kröger, D. G., & Kisters, A. (2014). Rock bed storage for solar thermal power plants: Rock characteristics, suitability, and availability. *Solar Energy Materials and Solar Cells*, 126, 170–183. <https://doi.org/10.1016/j.solmat.2014.03.030>
- Alva, G., Liu, L., Huang, X., & Fang, G. (2017). Thermal energy storage materials and systems for solar energy applications. *Renewable and Sustainable Energy Reviews*, 68, 693-706. <https://doi.org/https://doi.org/10.1016/j.rser.2016.10.021>
- Alzahrani, A. M., Lasheen, E. S. R., & Rashwan, M. A. (2022). Relationship of Mineralogical Composition to Thermal Expansion, Spectral Reflectance, and Physico-Mechanical Aspects of Commercial Ornamental Granitic Rocks. *Materials*, 15(6), 2041. <https://www.mdpi.com/1996-1944/15/6/2041>
- ASTM. (2013). *Annual Book of ASTM Standards*. American Society for Testing and Materials. <https://books.google.co.tz/books?id=IJu2wwEACAAJ>
- Bal, L. M., Satya, S., & Naik, S. N. (2010). Solar dryer with thermal energy storage systems for drying agricultural food products: A review. *Renewable & Sustainable Energy Reviews*, 14, 2298-2314. <https://doi.org/doi:10.1016/j.rser.2010.04.014>
- Bal, L. M., Satya, S., Naik, S. N., & Meda, V. (2011). Review of solar dryers with latent heat storage systems for agricultural products. *Renewable and Sustainable Energy Reviews*, 15(1), 876-880. <https://doi.org/https://doi.org/10.1016/j.rser.2010.09.006>
- Banerjee, D. (2020). Aravalli craton and its mobile belts: An update. *Episodes Journal of International Geoscience*, 43(1), 88-108.
- Baron, A., Burke, A. L., Gratuze, B., & Chapdelaine, C. (2016). Characterization and origin of steatite beads made by Northern Iroquoians in the St. Lawrence Valley during the 15th and 16th centuries. *Journal of Archaeological Science: Reports*, 8, 323-334.
- Bataineh, K., & Gharaibeh, A. (2018). Optimal design for sensible thermal energy storage tank using natural solid materials for a parabolic trough power plant. *Solar Energy*, 171, 519-525. <https://doi.org/https://doi.org/10.1016/j.solener.2018.06.108>
- Begg, G., Griffin, W., Natapov, L., O'Reilly, S., Grand, S., O'Neill, C., . . . Bowden, P. (2009). The lithospheric architecture of Africa: Seismic tomography, mantle petrology, and tectonic evolution. *Geosphere*, 5, 23-50. <https://doi.org/10.1130/GES00179.1>
- Borodich, F. M., Bull, S. J., & Epshtein, S. A. (2015). Nanoindentation in studying mechanical properties of heterogeneous materials. *Journal of Mining Science*, 51(3), 470-476. <https://doi.org/10.1134/S1062739115030072>
- Bouvry, B., Carrión, A. J. F., Andújar, J., Veron, E., Ory, S., Brassamin, S., . . . Py, X. (2017). Mediterranean basin basalts as potential materials for thermal energy storage in concentrated solar plants. *Solar Energy Materials and Solar Cells*, 171, 50-59.
- Cabeza, L. F., Martorell, I., Miró, L., Fernández, A. I., & Barreneche, C. (2015). 1 - Introduction to thermal energy storage (TES) systems. In L. F. Cabeza (Ed.), *Advances in Thermal Energy Storage Systems* (pp. 1-28). Woodhead Publishing. <https://doi.org/https://doi.org/10.1533/9781782420965.1>
- Caraballo, A., Galán-Casado, S., Caballero, Á., & Serena, S. (2021). Molten Salts for Sensible

- Thermal Energy Storage: A Review and an Energy Performance Analysis. *Energies* 2021, 14, 1197.
- Chen, C., Zhu, C., Zhang, B., Tang, B., Li, K., Li, W., & Fu, X. (2021). Effect of Temperature on the Thermal Conductivity of Rocks and Its Implication for In Situ Correction. *Geofluids*, 2021, 6630236. <https://doi.org/10.1155/2021/6630236>
- Cuce, P. M. (2018). Box type solar cookers with sensible thermal energy storage medium: A comparative experimental investigation and thermodynamic analysis. *Solar Energy*, 166, 432-440. <https://doi.org/10.1016/j.solener.2018.03.077>
- Eddemani, A., Bammou, L., Tiskatine, R., Aharoune, A., Bouirden, L., & Ihlal, A. (2021). Evaluation of the thermal performance of the air-rock bed solar energy storage system. *International Journal of Ambient Energy*, 42(15), 1699-1707. <https://doi.org/10.1080/01430750.2019.1614982>
- El Alami, K., Asbik, M., & Agalit, H. (2020). Identification of natural rocks as storage materials in thermal energy storage (TES) system of concentrated solar power (CSP) plants – A review. *Solar Energy Materials and Solar Cells*, 217, 110599. <https://doi.org/10.1016/j.solmat.2020.110599>
- Fasquelle, T., Falcoz, Q., Neveu, P., Walker, J., & Flamant, G. (2017). Compatibility Study Between Synthetic Oil and Vitrified Wastes for Direct Thermal Energy Storage. *Waste and Biomass Valorization*, 8(3), 621-631. <https://doi.org/10.1007/s12649-016-9622-1>
- Frink, L., Glazer, D., & Harry, K. G. (2012). Canadian Arctic Soapstone Cooking Technology. *North American Archaeologist*, 33(4), 429-449. <https://doi.org/10.2190/NA.33.4.c>
- Fritz, H., Tenczer, V., Hauzenberger, C., Wallbrecher, E., Hoinkes, G., Muhongo, S., & Mogessie, A. (2005). Central Tanzanian tectonic map: a step forward to decipher Proterozoic structural events in the East African Orogen. *Tectonics*, 24(6).
- Gabert, G. (1990). Lithostratigraphic and tectonic setting of gold mineralization in the Archean cratons of Tanzania and Uganda, East Africa. *Precambrian Research*, 46(1-2), 59-69.
- Gil, A., Medrano, M., Martorell, I., Lázaro, A., Dolado, P., Zalba, B., & Cabeza, L. F. (2010). State of the art on high temperature thermal energy storage for power generation. Part 1—Concepts, materials and modellization. *Renewable and Sustainable Energy Reviews*, 14(1), 31-55. <https://doi.org/10.1016/j.rser.2009.07.035>
- Godfray, G., Kabohola, J., & Msabi, M. (2021). Sedimentology and compositional characteristics of siliciclastic and associated sediments in Ruvu basin: implication on paleo-depositional environment, provenance, and tectonic setting. *Geology, Ecology, and Landscapes*, 1-13. <https://doi.org/10.1080/24749508.2021.2022447>
- Godfray, G., Kabohola, J., & Msabi, M. (2022). Sedimentology and compositional characteristics of siliciclastic and associated sediments in Ruvu basin: implication on paleo-depositional environment, provenance, and tectonic setting. *Geology, Ecology, and Landscapes*, 1-13.
- Grirate, H., Zari, N., Elamrani, I., Couturier, R., Elmchaouri, A., Belcadi, S., & Tochon, P. (2014). Characterization of several Moroccan rocks used as filler material for thermal energy storage in CSP power plants. *Energy Procedia*, 49, 810-819.
- GST. (2015). *Explanatory notes for the minerogenic map of Tanzania*.
- Haldar, S. K., & Tišljär, J. (2014). Chapter 4 - Igneous Rocks. In S. K. Haldar & J. Tišljär (Eds.), *Introduction to Mineralogy and Petrology* (pp. 93-120). Elsevier. <https://doi.org/10.1016/B978-0-12-408133-8.00004-3>
- Hänchen, M., Brückner, S., & Steinfeld, A. (2011). High-temperature thermal storage using a packed bed of rocks – Heat transfer analysis and experimental validation. *Applied Thermal Engineering*, 31(10), 1798-1806. <https://doi.org/10.1016/j.applthermaleng.2010.10.034>
- Hartlieb, P., Toifl, M., Kuchar, F., Meisels, R., & Antretter, T. (2016). Thermo-physical properties of selected hard rocks and their relation to microwave-assisted comminution. *Minerals Engineering*, 91, 34-41. <https://doi.org/10.1016/j.mineng.2015.11.008>
- Herrmann, U., & Kearney, D. W. (2002). Survey of Thermal Energy Storage for Parabolic Trough

- Power Plants. *Journal of Solar Energy Engineering*, 124(2), 145-152. <https://doi.org/10.1115/1.1467601>
- Hrifech, S., Agalit, H., Bennouna, E. G., Jarni, A., Mouguina, E. M., & Mimet, A. (2019). Preliminary characterizations of natural rocks as storage materials for a medium range temperature TES. *AIP Conference Proceedings*, 2123(1), 020091. <https://doi.org/10.1063/1.5117018>
- Huhta, A. (2019). *Diversity of soapstones: Classification and thermal behavior* (Publication Number Ser. A, No. 39) University of Oulu]. Oulun yliopiston geotieteiden julkaisu.
- Huhta, A., Kärki, A., & Hanski, E. (2016). A new method for testing thermal shock resistance properties of soapstone-Effects of microstructures and mineralogical variables. *Bulletin of the Geological Society of Finland*, 88(1).
- Huhta, A., Tuisku, P., Balic-Zunic, T., & Kärki, A. (2019). Magnesite soapstone in use of fire chamber constructions: composition and structure adaptation. *Bulletin of the Geological Society of Finland*, 91.
- James, D., & Fouch, M. (2002). Formation and evolution of Archaean cratons: Insights from southern Africa. *Geological Society, London, Special Publications*, 199, 1-26. <https://doi.org/10.1144/GSL.SP.2002.199.01.01>
- Jones, M. (2003). Thermal properties of stratified rocks from Witwatersrand gold mining areas. *Journal of the Southern African Institute of Mining and Metallurgy*, 103(3), 173-185.
- Kabete, J., McNaughton, N., Groves, D., & Mruma, A. H. (2012). Reconnaissance SHRIMP U–Pb zircon geochronology of the Tanzania Craton: evidence for Neoproterozoic granitoid–greenstone belts in the Central Tanzania Region and the Southern East African Orogen. *Precambrian Research*, 216, 232-266.
- Kant, K., Shukla, A., Sharma, A., Kumar, A., & Jain, A. (2016). Thermal energy storage based solar drying systems: A review. *Innovative food science & emerging technologies*, 34, 86-99.
- Khare, S., Dell'Amico, M., Knight, C., & McGarry, S. (2013). Selection of materials for high temperature sensible energy storage. *Solar Energy Materials and Solar Cells*, 115, 114-122. <https://doi.org/10.1016/j.solmat.2013.03.009>
- Koçak, B., Fernandez, A. I., & Paksoy, H. (2020). Review on sensible thermal energy storage for industrial solar applications and sustainability aspects. *Solar Energy*, 209, 135-169. <https://doi.org/10.1016/j.solener.2020.08.081>
- Koçak, B., Fernández, A. I., & Paksoy, H. (2021). Characterization of demolition waste powder to be processed as sensible thermal energy storage material. *Solar Energy Materials and Solar Cells*, 230, 111283. <https://doi.org/10.1016/j.solmat.2021.111283>
- Kora, A. J. (2020). Traditional soapstone storage, serving, and cookware used in the Southern states of India and its culinary importance. *Bulletin of the National Research Centre*, 44(1), 83. <https://doi.org/10.1186/s42269-020-00340-w>
- Laing, D., Steinmann, W.-D., Tamme, R., & Richter, C. (2006). Solid media thermal storage for parabolic trough power plants. *Solar Energy*, 80(10), 1283-1289. <https://doi.org/10.1016/j.solener.2006.06.003>
- Lemenkova, P. (2022). Tanzania Craton, Serengeti Plain and Eastern Rift Valley: mapping of geospatial data by scripting techniques. *Estonian Journal of Earth Sciences*, 71, 61-79. <https://doi.org/10.3176/earth.2022.05>
- Li, B., Ju, F., Xiao, M., & Ning, P. (2019). Mechanical stability of granite as thermal energy storage material: An experimental investigation. *Engineering Fracture Mechanics*, 211, 61-69. <https://doi.org/10.1016/j.engfracmech.2019.02.008>
- Ma, Z., Pathegama Gamage, R., & Zhang, C. (2020). Application of nanoindentation technology in rocks: a review. *Geomechanics and Geophysics for Geo-Energy and Geo-Resources*, 6(4), 60. <https://doi.org/10.1007/s40948-020-00178-6>
- Manya, S., & Maboko, M. A. H. (2016). Generation of Palaeoproterozoic tonalites and associated high-K granites in southwestern Tanzania by partial melting of underplated mafic crust in

- an intracontinental setting: Constraints from geochemical and isotopic data. *Lithos*, 260, 120-133. <https://doi.org/https://doi.org/10.1016/j.lithos.2016.05.011>
- Maqsood, A., Kamran, K., & Gul, I. H. (2004). Prediction of thermal conductivity of granite rocks from porosity and density data at normal temperature and pressure: in situ thermal conductivity measurements. *Journal of Physics D: Applied Physics*, 37(24), 3396.
- Micallef, T. (2019). *Earthquake detection and localisation using the NARS-Botswana data* MSc thesis). Utrecht University. Retrieved from [https://seismologie.sites ...](https://seismologie.sites...)].
- Moeller, A., Appel, P., Mezger, K., & Schenk, V. (1995). Evidence for a 2 Ga subduction zone: Eclogites in the Usagaran belt of Tanzania. *Geology*, 23. [https://doi.org/10.1130/0091-7613\(1995\)023<1067:EFAGSZ>2.3.CO;2](https://doi.org/10.1130/0091-7613(1995)023<1067:EFAGSZ>2.3.CO;2)
- Mori, K., Tsujimori, T., & Boniface, N. (2018). Finding of talc–and kyanite–bearing amphibolite from the Paleoproterozoic Usagaran Belt, Tanzania. *Journal of Mineralogical and Petrological Sciences*, 113(6), 316-321.
- Muh, E., & Tabet, F. (2019). Comparative analysis of hybrid renewable energy systems for off-grid applications in Southern Cameroons. *Renewable energy*, 135, 41-54.
- Nahhas, T., Py, X., & Sadiki, N. (2019). Experimental investigation of basalt rocks as storage material for high-temperature concentrated solar power plants. *Renewable and Sustainable Energy Reviews*, 110, 226-235.
- Navarro, M. E., Martínez, M., Gil, A., Fernández, A. I., Cabeza, L. F., Olives, R., & Py, X. (2012). Selection and characterization of recycled materials for sensible thermal energy storage. *Solar Energy Materials and Solar Cells*, 107, 131-135. <https://doi.org/https://doi.org/10.1016/j.solmat.2012.07.032>
- Oliver, W. C., & Pharr, G. M. (2011). An improved technique for determining hardness and elastic modulus using load and displacement sensing indentation experiments. *Journal of Materials Research*, 7(6), 1564-1583. <https://doi.org/10.1557/JMR.1992.1564>
- Oyedotun, T. D. T. (2018). X-ray fluorescence (XRF) in the investigation of the composition of earth materials: a review and an overview. *Geology, Ecology, and Landscapes*, 2(2), 148-154. <https://doi.org/10.1080/24749508.2018.1452459>
- Pirinen, H. (2005). Mineralogy of soapstone.
- Price, H., Lu'pfert, E., Kearney, D., Zarza, E., Cohen, G., Gee, R., & Mahoney, R. (2002). Advances in Parabolic Trough Solar Power Technology. *Journal of Solar Energy Engineering*, 124(2), 109-125. <https://doi.org/10.1115/1.1467922>
- Priem, H. N. A., Boelrijk, N. A. I. M., Hebeda, E. H., Verdurmen, E. A. T., Verschure, R. H., Oen, I. S., & Westra, L. (1979). Isotopic age determinations on granitic and gneissic rocks from the Ubendian-Usagaran system in southern Tanzania. *Precambrian Research*, 9(3), 227-239. [https://doi.org/https://doi.org/10.1016/0301-9268\(79\)90004-4](https://doi.org/https://doi.org/10.1016/0301-9268(79)90004-4)
- REN21. (2021). *Renewables 2021 Global Status Report*. U. N. E. Programme. <https://www.unep.org/resources/report/renewables-2021-global-status-report>
- Ring, U., Kröner, A., & Toulkeridis, T. (1997). Palaeoproterozoic granulite-facies metamorphism and granitoid intrusions in the Ubendian-Usagaran Orogen of northern Malawi, east-central Africa. *Precambrian Research*, 85(1), 27-51. [https://doi.org/https://doi.org/10.1016/S0301-9268\(97\)00028-4](https://doi.org/https://doi.org/10.1016/S0301-9268(97)00028-4)
- Rybacki, E., Reinicke, A., Meier, T., Makasi, M., & Dresen, G. (2015). What controls the mechanical properties of shale rocks? – Part I: Strength and Young's modulus. *Journal of Petroleum Science and Engineering*, 135, 702-722. <https://doi.org/https://doi.org/10.1016/j.petrol.2015.10.028>
- Sawada, H., Isozaki, Y., Sakata, S., Hirata, T., & Maruyama, S. (2018). Secular change in lifetime of granitic crust and the continental growth: A new view from detrital zircon ages of sandstones. *Geoscience Frontiers*, 9(4), 1099-1115.
- Shang, X., Zhang, Z., Xu, X., Liu, T., & Xing, Y. (2019). Mineral Composition, Pore Structure, and Mechanical Characteristics of Pyroxene Granite Exposed to Heat Treatments. *Minerals*, 9(9).

- Singh, H., Saini, R., & Saini, J. (2010). A review on packed bed solar energy storage systems. *Renewable and Sustainable Energy Reviews*, 14(3), 1059-1069.
- Sommer, H., & Kröner, A. (2013). Ultra-high temperature granulite-facies metamorphic rocks from the Mozambique belt of SW Tanzania. *Lithos*, 170, 117-143.
- Srinivasan, S., Dodson, D., Charles, M. B. J., Wallen, S. L., Albarelli, G., Kaushik, A., . . . Dhau, J. (2020). Energy Storage in Earth-Abundant Dolomite Minerals. *Applied Sciences*, 10(19), 6679.
- Srivastava, P., Krishna, A., Jawed, S., & Sarkhel, P. (2020). Quantitative minerological analysis of some granite rocks of deoghar jharkhand. *Earth Sci. Res*, 9, 30.
- Strecker, K., Panzera, T., Sabariz, A., & Miranda, J. (2010). The effect of incorporation of steatite wastes on the mechanical properties of cementitious composites. *Materials and structures*, 43(7), 923-932.
- Sun, K., Zhang, L.-l., Zhao, Z.-d., He, F.-q., He, S.-f., Wu, X.-y., . . . Ren, X.-d. (2018). Episodic crustal growth in the Tanzania Craton: evidence from Nd isotope compositions. *China Geology*, 1(2), 210-224. <https://doi.org/https://doi.org/10.31035/cg2018025>
- Suresh, C., & Saini, R. P. (2020). Review on solar thermal energy storage technologies and their geometrical configurations [<https://doi.org/10.1002/er.5143>]. *International Journal of Energy Research*, 44(6), 4163-4195. <https://doi.org/https://doi.org/10.1002/er.5143>
- Tankard, A. J., Martin, M., Eriksson, K., Hobday, D., Hunter, D., & Minter, W. (2012). *Crustal evolution of southern Africa: 3.8 billion years of earth history*. Springer Science & Business Media.
- Tatsidjodoung, P., Le Pierrès, N., & Luo, L. (2013). A review of potential materials for thermal energy storage in building applications. *Renewable and Sustainable Energy Reviews*, 18, 327-349. <https://doi.org/https://doi.org/10.1016/j.rser.2012.10.025>
- Thomas, R. J., Roberts, N. M. W., Jacobs, J., Bushi, A. M., Horstwood, M. S. A., & Mruma, A. (2013). Structural and geochronological constraints on the evolution of the eastern margin of the Tanzania Craton in the Mpwapa area, central Tanzania. *Precambrian Research*, 224, 671-689. <https://doi.org/https://doi.org/10.1016/j.precamres.2012.11.010>
- Tiskatine, R., Oaddi, R., El Cadi, R. A., Bazgaou, A., Bouriden, L., Aharoune, A., & Ihlal, A. (2017). Suitability and characteristics of rocks for sensible heat storage in CSP plants. *Solar Energy Materials and Solar Cells*, 169, 245-257.
- Valentine, G. A., & Connor, C. B. (2015). Chapter 23 - Basaltic Volcanic Fields. In H. Sigurdsson (Ed.), *The Encyclopedia of Volcanoes (Second Edition)* (pp. 423-439). Academic Press. <https://doi.org/https://doi.org/10.1016/B978-0-12-385938-9.00023-7>
- Veizer, J., & Mackenzie, F. T. (2014). 9.15 - Evolution of Sedimentary Rocks. In H. D. Holland & K. K. Turekian (Eds.), *Treatise on Geochemistry (Second Edition)* (pp. 399-435). Elsevier. <https://doi.org/https://doi.org/10.1016/B978-0-08-095975-7.00715-4>
- Vindel, J. M., & Polo, J. (2014). Intermittency and variability of daily solar irradiation. *Atmospheric Research*, 143, 313-327. <https://doi.org/https://doi.org/10.1016/j.atmosres.2014.03.001>
- Vosteen, H.-D., & Schellschmidt, R. (2003). Influence of temperature on thermal conductivity, thermal capacity and thermal diffusivity for different types of rock. *Physics and Chemistry of the Earth, Parts A/B/C*, 28(9), 499-509. [https://doi.org/https://doi.org/10.1016/S1474-7065\(03\)00069-X](https://doi.org/https://doi.org/10.1016/S1474-7065(03)00069-X)
- Wang, K., Qin, Z., Tong, W., & Ji, C. (2020). Thermal energy storage for solar energy utilization: Fundamentals and applications. *Resources, Challenges and Applications*, 415.
- Yavuz, H., Demirdag, S., & Caran, S. (2010). Thermal effect on the physical properties of carbonate rocks. *International Journal of Rock Mechanics and Mining Sciences*, 47(1), 94-103.
- Zhang, H., Baeyens, J., Cáceres, G., Degève, J., & Lv, Y. (2016). Thermal energy storage: Recent developments and practical aspects. *Progress in Energy and Combustion Science*, 53, 1-40. <https://doi.org/https://doi.org/10.1016/j.pecs.2015.10.003>

- Zheng, H., Schenk, J., Spreitzer, D., Wolfinger, T., & Daghagheleh, O. (2021). Review on the Oxidation Behaviors and Kinetics of Magnetite in Particle Scale [<https://doi.org/10.1002/srin.202000687>]. *steel research international*, 92(8), 2000687. <https://doi.org/https://doi.org/10.1002/srin.202000687>
- Zhu, Z., Tian, H., Jiang, G., & Dou, B. (2022). Effects of high temperature on rock bulk density. *Geomechanics and Geoengineering*, 17(2), 647-657. <https://doi.org/10.1080/17486025.2020.1827169>

APPENDICES

Appendix 1: Data and Citation for the most common used TES materials

Material	Density	Thermal Conductivity	Specific Heat	Thermal Capacity	Max. operating temperature	Reference
	g/cm ³	W/mK	J/kgK	kJ/m ³ K	°C	
Concrete	2.2-2.7	0.9-2	750-1130	1680-3005	400-500	Gil et al. (2010), Tiskatine et al. (2017)
HT concrete	2.8	1-2.0	916	2519	400	Tiskatine et al. (2017), (El Alami <i>et al.</i> , 2020) Suresh and Saini (2020)
High alumina concrete	2.4	0.2	980	2352	1800	Tiskatine et al. (2017), Khare et al. (2013)
Reinforced concrete	2.2	1.5	850	1870	400	Tiskatine et al. (2017), Gil et al. (2010)
Cement mortar	1.9-2	0.6-0.7	642	1194-1309		Tiskatine et al. (2017),
Castable ceramic	3.5	1.35-1.4	866	3031	400	Tiskatine et al. (2017), Bataineh and Gharaibeh (2018)
Brick	1.7-1.8	0.5-0.7	840	1419-1512	400	Tiskatine et al. (2017), Suresh and Saini (2020), (Tatsidjodoun <i>et al.</i> , 2013)
Brick magnesia	3	5-5.1	1130-1150	3390-3450	1200	Tiskatine et al. (2017), Zhang et al. (2016)
Silica fire bricks	1.8	1.5	1000	1820	700	Tiskatine et al. (2017), Gil et al. (2010)
Copper	8.3-9	372-385	383-419	3178-3729	1400	Tiskatine et al. (2017), Suresh and Saini (2020)

Cast iron	7.2-7.9	29.3-73	465-837	3348-6612	400	Tiskatine et al. (2017), Zhang et al. (2016)
Aluminium	2.7	204-238.4	896-945	2419-2551	1400	Tiskatine et al. (2017), Suresh and Saini (2020)
Lead	11.3	35.3	131	1485	1400	Tiskatine et al. (2017), Suresh and Saini (2020)
Cofalit	3.1	1.4-2.7	800-1034	2496-3226	1100	Tiskatine et al. (2017), Koçak et al. (2021)
Graphite	2.2-2.3	122-155	401-610	882-1378	1600	Tiskatine et al. (2017), (Khare <i>et al.</i> , 2013)
Sodium chloride	2.2	6.5-7	850-860	1836-1861	500	Tiskatine et al. (2017), Gil et al. (2010)
Molten salts	0.5-2.6	0.2-2	1500	1350-3900	500-600	Tiskatine et al. (2017), Allen et al. (2014)
Solar salt	1.9	0.5	1495	2825	565	Tiskatine et al. (2017), Suresh and Saini (2020)
Mineral oil	0.8	0.1	2600	2002	400	Tiskatine et al. (2017), Suresh and Saini (2020), Alva et al. (2017)
Synthetic oil	0.9	0.1	2100-2300	1890-2070	350	Tiskatine et al. (2017), Allen et al. (2014)
Liquid sodium	0.9	71	1300	1105	530	Tiskatine et al. (2017), Allen et al. (2014)
Water	1	0.6	4187	4174	90	Tiskatine et al. (2017), Suresh and Saini (2020)
Demolition wastes	2.855	0.53	1457	4160	700	Koçak et al. (2021)
Sand	1.7-2.2	2	910-1180	1547-2596	550	Suresh and Saini (2020),

						Alva et al. (2017)
Nitrate salts	1.87	0.52	1600	2992	565	Zhang et al. (2016)
Nitrite salts	1.82	0.57	1500	2730	450	Zhang et al. (2016)

RESEARCH OUTPUTS

(i) Publication

Kakoko, L. D., Jande, Y. A. C., & Kivevele, T. (2023). Experimental Investigation of Soapstone and Granite Rocks as Energy-Storage Materials for Concentrated Solar Power Generation and Solar Drying Technology. *ACS Omega*, 8(21), 18554-18565.

(ii) Poster Presentation